Earth-Science Reviews 221 (2021) 103785

Contents lists available at ScienceDirect

Earth-Science Reviews

journal homepage: www.elsevier.com/locate/earscirev

Miocene paleoceanographic evolution of the Mediterranean area and carbonate production changes: A review

Irene Cornacchia [a,*], Marco Brandano [b,c], Samuele Agostini [a]

[a] Istituto di Geoscienze e Georisorse (IGG), CNR, Via G. Moruzzi 1, 56124 Pisa, Italy
[b] Dipartimento di Scienze della Terra, Sapienza Università di Roma, P.le Aldo Moro 5, 00185 Roma, Italy
[c] Istituto di Geologia Ambientale e Geoingegneria (IGAG), CNR, Sez. Sapienza, Dipartimento Scienze della Terra, P.le Aldo Moro 5, 00185 Roma, Italy

ARTICLE INFO

Keywords:
Carbonate platforms
Mediterranean
Miocene
Sr isotopes
Nd isotopes
paleoceanography

ABSTRACT

Miocene is a key interval in the global climate evolution as well as in the geodynamic evolution of the Mediterranean basin. Therefore, global and regional factors controlled Miocene Mediterranean oceanography, which, in turn, affected carbonate production. In this work, we review the Miocene paleocenographic evolution of the Mediterranean starting from its Sr and Nd isotope records. Secondly, we discuss Mediterranean shallow-water carbonate production changes to identify the role of oceanographic conditions in controlling carbonate systems' evolution.

During Aquitanian, Sr and Nd isotope records attest an open Mediterranean, mainly fed by the Indian Ocean. From the late Burdigalian, the intermittent connection with the Indian Ocean changed the overall circulation in the basin, leading to higher residence time of waters and smaller water exchanges with the adjacent oceans. In this newly established paleoceanographic framework, regional factors such as volcanism, significantly affected Mediterranean seawater chemistry. Local tectonics led to the development of small sub-basins in the Eastern Mediterranean, characterized by restricted water exchanges from the Tortonian in the easternmost part, to the early Messinian, as attested by the deviation of the Sr isotope record of the proto-Adriatic basin.

Larger Benthic Foraminifera (LBF) assemblages dominated carbonate production in the Aquitanian, while they were the most affected by the Indo-Pacific closure, showing a demise after the Burdigalian. With the LBF demise, red algae and bryozoans dominated carbonate ramps from the middle Miocene to the Tortonian. Bryozoans in particular spread during the Monterey Event, favoured by global and regional factors. During early to middle Miocene, corals formed mounds in the oligophotic zone or coral carpets controlled by local conditions. Conversely, in the late Tortonian-early Messinian, they developed as huge reef complexes in the Western and Central Mediterranean, with the exception of small restricted sub-basins, such as the proto-Adriatic basin, where red algae and small benthic foraminifera persisted.

1. Introduction

Carbonate producing biota are sensitive to multiple factors, such as water temperature and nutrient content, light penetration, type of substrate, water circulation patterns, stratification of the water column and hydrodynamic regime (Hallock and Schlager, 1986; James, 1997; Mutti and Hallock, 2003; Pomar et al., 2004; Schlager, 2005). Overall, these parameters are controlled by global climate and geodynamic at different time and spatial scales.

Oceanography and current patterns are key aspects in determining ecological requirements of biota producing carbonate sediment. Sr and Nd isotope systematics are reliable proxies of paleoceanographic changes, which have been increasingly used in different settings and stratigraphic intervals (Kocsis et al., 2008; Dera et al., 2009; Schildgen et al., 2014; Batenburg et al., 2018; Cornacchia et al., 2018; Coxall et al., 2018).

The $^{87}Sr/^{86}Sr$ ratio in seawater depends on weathering, that tends to increase the ratios towards higher values, and volcanism, that injects in seawater high amounts of light ^{86}Sr, lowering the overall Sr isotope ratios. Sr residence time in seawater (10^6 years) is several orders of magnitude longer than oceanic circulation (10^3 years). Therefore, considering geological time scales, the Sr isotope record of the global

* Corresponding author.
E-mail address: irene.cornacchia@igg.cnr.it (I. Cornacchia).

https://doi.org/10.1016/j.earscirev.2021.103785
Received 4 May 2021; Received in revised form 31 July 2021; Accepted 23 August 2021
Available online 25 August 2021

ocean is homogeneous, as attested by the global Sr reference curve established for the entire Phanerozoic (McArthur et al., 2001, 2012 and references therein). On the contrary, closed, semi-closed or restricted basins might show a deviation of their Sr isotope record with respect to the contemporary global ocean record (Ingram and Sloan, 1992; Kocsis et al., 2008; Schildgen et al., 2014; Cornacchia et al., 2017, 2018). In those cases, the amount and direction (lighter vs heavier Sr isotope ratios) of the deviation are good evidences of the isolation or restriction of the basin, as well as the main controlling factors on the seawater chemistry (weathering vs volcanism).

$^{143}Nd/^{144}Nd$ ratio of marine carbonates is a good proxy for paleoceanographic reconstructions since it shows a strong provinciality character. In fact, a distinct Nd isotope signature characterizes every ocean (Bertram and Elderfield, 1993; O'nions et al., 1998; Frank, 2002; Lacan et al., 2012), due to the short residence time of Nd in seawater (200–1550 years; Piepgras et al., 1979). Therefore, the lithologies cropping out in the drainage areas feeding a selected basin, as well as circulation patterns and water exchanges, control the Nd isotope signature of a basin (Goldstein and Jacobsen, 1987). Old continental crust tends to have very low ε_{Nd} isotope values, while young volcanism shows a more radiogenic signal. Therefore, the Northern Atlantic Nd isotope record, that drains the old Canadian Shield (Piepgras and Wasserburg, 1987), is significantly lower than the Pacific record (Piepgras and Jacobsen, 1988), influenced by recent volcanism. Lastly, smaller basins, such as the Mediterranean, have a Nd isotope signature that is partly influenced by the inflow of the adjacent oceans, and partly results from the regional geology and that of the drainage basins of the main rivers (Frost et al., 1986; Spivack and Wasserburg, 1988; Henry et al., 1994; Tachikawa et al., 2004).

In this work, we propose a review of the Miocene paleocenographic evolution of the Mediterranean area starting from its Sr and Nd isotope records. Secondly, we discuss Mediterranean shallow-water carbonate production changes to identify the role of oceanographic conditions in controlling carbonate systems' evolution.

2. The Miocene global climate evolution and C-cycle perturbations

The Miocene is a key interval of the global climate evolution of the Earth (Fig. 1). Overall, it is characterized by a long-term cooling trend, showing an unstable Antarctic ice sheet between the early to middle Miocene, to a progressively stable Antarctica, enhanced circulation patterns, and the onset of the Northern Hemisphere glaciation at the end of the Miocene (Zachos et al., 2001; Lear et al., 2004; Liebrand et al., 2011; Holbourn et al., 2018). The base of the Aquitanian is marked by a positive $\delta^{18}O$ shift in the deep ocean record, named Mi-1 Event (Fig. 1A, Miller et al., 1991). This shift attests a moment of expansion of the Antarctica ice sheet, which reached the 120% of the nowadays volume (Pekar and DeConto, 2006), and consequent sea-level drop (Fig. 1B). This cooling trend changes in the late Burdigalian-Langhian interval, characterized instead by a long global warming phase, marked by a negative shift in the oxygen isotope record, and known as the Middle Miocene Climatic Optimum (Fig. 1A, MMCO, 17–14.7 Ma, Zachos et al., 2001, 2008; You et al., 2009; Super et al., 2018, 2020). The MMCO represents the warmest time interval of the past 35 Ma (Zachos et al., 2008), after which a stepped cooling phase developed globally (Zachos et al., 2001; Westerhold et al., 2005; Holbourn et al., 2013), strong latitudinal temperature gradients established (Herbert et al., 2016), and monsoon intensified (Holbourn et al., 2018). Messinian is in fact characterized by significant lower sea surface temperatures globally and a more arid climate (Tzanova et al., 2015; Herbert et al., 2016).

The global climate evolution and ocean circulation changes are mutually related to carbon cycle dynamics and perturbations. The Miocene carbon isotope record of deep ocean shows different positive spikes linked to increased organic carbon burial rates with respect to carbonate precipitation (Fig. 1C, Zachos et al., 2001). The first positive $\delta^{13}C$ shift is attested in the early Aquitanian, contemporary to the Mi-1 Event, and it has been linked to an excess of nutrients into surface waters due to increased weathering and enhanced circulation (Zachos et al., 2001; Lear et al., 2004). Conversely, a long-term positive carbon isotope excursion is recorded during the MMCO and named Monterey Event (Fig. 1C). It is named after the type locality of Monterey (California, USA), where large amounts of organic carbon are stored in a hemipelagic carbonate succession (Vincent and Berger, 1985; Woodruff and Savin, 1991). Six carbon isotope maxima (CMs), orbitally tuned, form the Monterey Carbon Isotope Excursion (MCIE, Holbourn et al., 2004, 2007). Lastly, at the Serravallian-Tortonian boundary another positive carbon isotope shift is recorded in the global ocean record, and named CM7 (Carbon Maximum 7, Holbourn et al., 2004). Conversely with respect to the six CMs belonging to the Monterey Excursion, the CM7 has

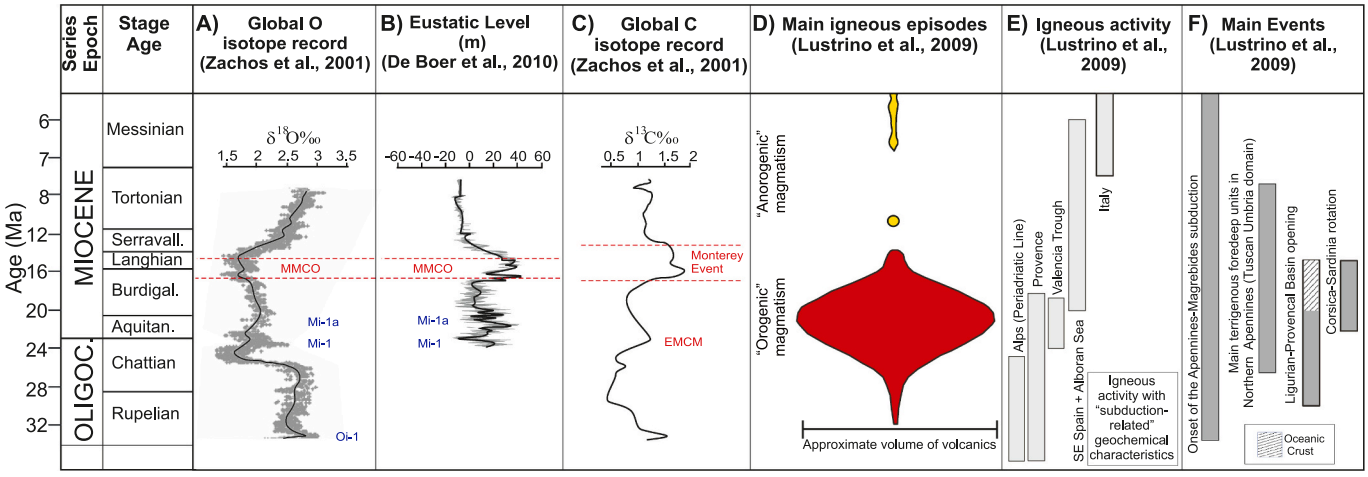

Fig. 1. Chrono-diagram showing the main global climatic, climate-related and regional geodynamic events of the Miocene. A) Global $\delta^{18}O$ isotope record of the Oligocene-Miocene time interval (modified after Zachos et al., 2001); MMCO = Middle Miocene Climatic Optimum. (B) Eustatic sea level record during Miocene (modified from De Boer et al., 2010). (C) Global $\delta^{13}C$ isotope record of the Oligocene-Miocene time interval (modified after Zachos et al., 2001). EMCM = Early Miocene Carbon Maximum. (D) Qualitative volumes of the subduction-related and anorogenic-type volcanism developed in Sardinia during Miocene (modified and redrawn after Lustrino et al., 2009); (E) Spatio-temporal distribution of the main igneous activity events with subduction-related characteristics in the Central Western Mediterranean during Miocene (modified and redrawn after Lustrino et al., 2009); (F) Main geodynamic events occurred in the Western and Central Mediterranean during Miocene (modified and redrawn after Lustrino et al., 2009).

been recorded during a global cooling phase and has been linked to enhanced ocean circulation, redistribution of upwelling and therefore increased nutrient content into surface water (Cramer et al., 2009; Holbourn et al., 2013). After the CM7, the carbon isotope curve shows a decreasing trend, testifying for increasing oligotrophic conditions of waters on a global scale (Zachos et al., 2001) as well as for the Mediterranean basin (Kouwenhoven and Van der Zwaan, 2006).

3. The Mediterranean geodynamic evolution

The Mediterranean area is the result of the complex interplay between the African, Arabian and Eurasian plates, together with several other microplates, such as Anatolia and Adria (Fig. 2; Carminati and Doglioni, 2005). The Malta escarpment separates the Eastern from the Central-Western portion of the Mediterranean basin.

The evolution of Eastern Mediterranean was determined by the collision between Africa and the Greek and Anatolia microplates. The collision, started in the Late Cretaceous, was followed by an extensional tectonics in the Aegean area due to differential northeastern migrations of the Greek and Anatolian microplates (Agostini et al., 2010 and references therein). In this context, the Aegean basin is characterized by an extensional tectonics that progressively migrated towards SW from Eocene to Recent. Furthermore, significant post-orogenic calc-alkaline volcanism developed in the Aegean basin from Miocene to Recent (Doglioni et al., 2002; Agostini et al., 2010). Lastly, the collision between the Arabia and Anatolia, linked to the relative movements between Africa and Arabia plates, led to the development of significant uplift in the Anatolian region in the late Miocene, creating a very heterogeneous paleogeographic evolution of the Eastern Mediterranean (Schildgen et al., 2012).

The Central-Western Mediterranean area developed mostly during the Neogene after the inversion of the Alpine-Betic subduction and the development of the westward-dipping Apennines-Maghrebide subduction (Carminati and Doglioni, 2005). The Apennines orogenesis consists of a west-directed subduction of the Neotethys under the margin of the European plate (Carminati et al., 2012). This west-directed subduction resulted in an eastward migration of the compressional wave and accretionary wedge during Neogene, and a contemporary extensional tectonics in the back-area (Fig. 1D–F, Gueguen et al., 1998; Carminati and Doglioni, 2005). The propagation of the Apenninic fronts and back-arc migration led to the restriction of the proto-Adriatic basin in the eastern sector of the Central Mediterranean area, and the opening and widening of continental troughs (Valencia) and oceanic basins (Thyrrenian) in the Western and Central Mediterranean (Fig. 1F, Carminati et al., 2010). Furthermore, a strong subduction-related volcanism developed in the Western Mediterranean during Miocene, followed by an anorogenic-type volcanism in the Western and Central Mediterranean from late Miocene to Recent (Fig. 1D–E, Lustrino et al., 2009).

Lastly, the Westernmost Mediterranean was mostly controlled in the Neogene by the counterclockwise rotation of the Iberian Plate linked to the opening of the Biscay Basin (Carminati and Doglioni, 2005), which affected severely local paleogeography as well as Mediterranean-Atlantic water exchanges.

4. The Miocene Mediterranean paleogeographic and paleoceanographic evolution

The Mediterranean basin evolved into its actual shape and physiography mostly during Miocene (Fig. 3). In the early Miocene, in fact, the Mediterranean was open to both the Atlantic and the Indo-Pacific Oceans (Fig. 3A, Rögl, 1999; Meulenkamp and Sissingh, 2003; Popov et al., 2004). The Mediterranean and the Indian Ocean, in particular, exchanged through the Indian Gateway or Mesopotamian Seaway, a sub-basin developed north of the Arabian Plate (Fig. 3A, Popov et al., 2004). Furthermore, Cao et al. (2017), analyzing marine fossil records of the Red Sea and Eastern Mediterranean basin, propose a second open connection through the Red Sea, active at least until the Aquitanian. Paleoceanographic models show that, with a deep Indian Gateway, a significant shallow water inflow entered in the Mediterranean and circulated westward (de la Vara et al., 2013; de La Vara and Meijer, 2016). Furthermore, different models state that a deep Indian Gateway was necessary to keep an efficient estuarine circulation between the Mediterranean and the Atlantic Ocean (Karami et al., 2009; de La Vara and Meijer, 2016).

Cornacchia et al. (2018) analysed the Sr isotope record of the hemipelagic Umbria-Marche basin (Central Mediterranean), showing that in the early Aquitanian the Sr isotope record fitted with the global Ocean (Fig. 4A, McArthur and Howarth, 2004). This is in agreement with the

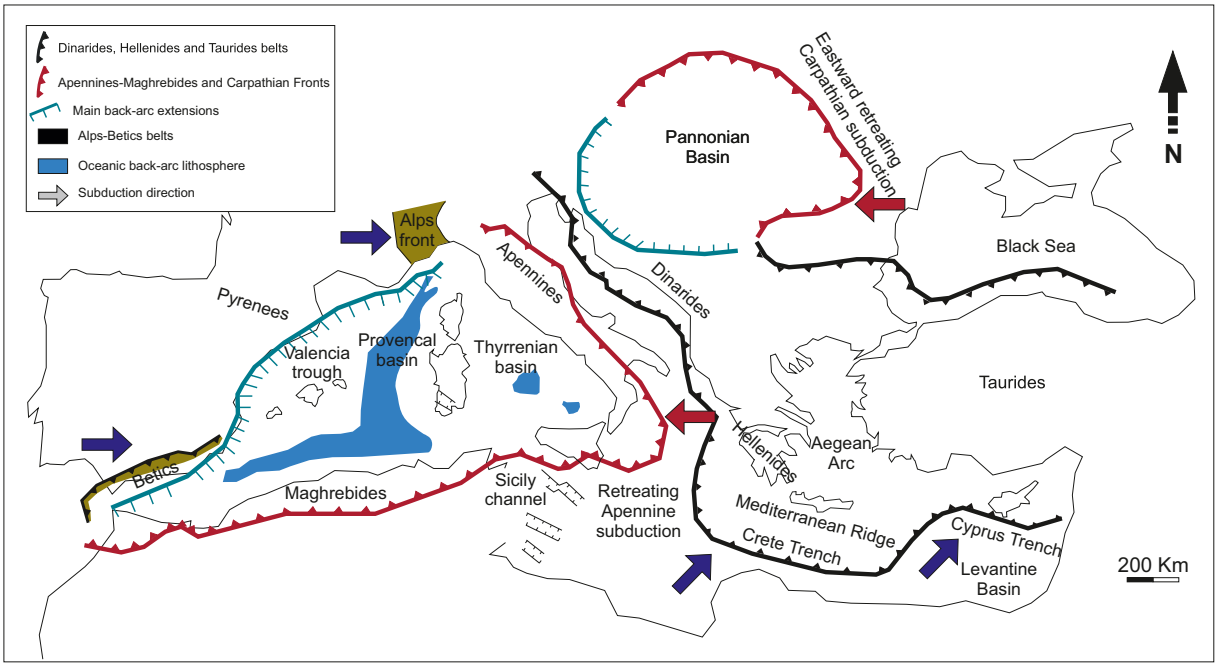

Fig. 2. Simplified geodynamic sketch of the Mediterranean modified and redrawn from Agostini et al. (2010), after Carminati and Doglioni (2005).

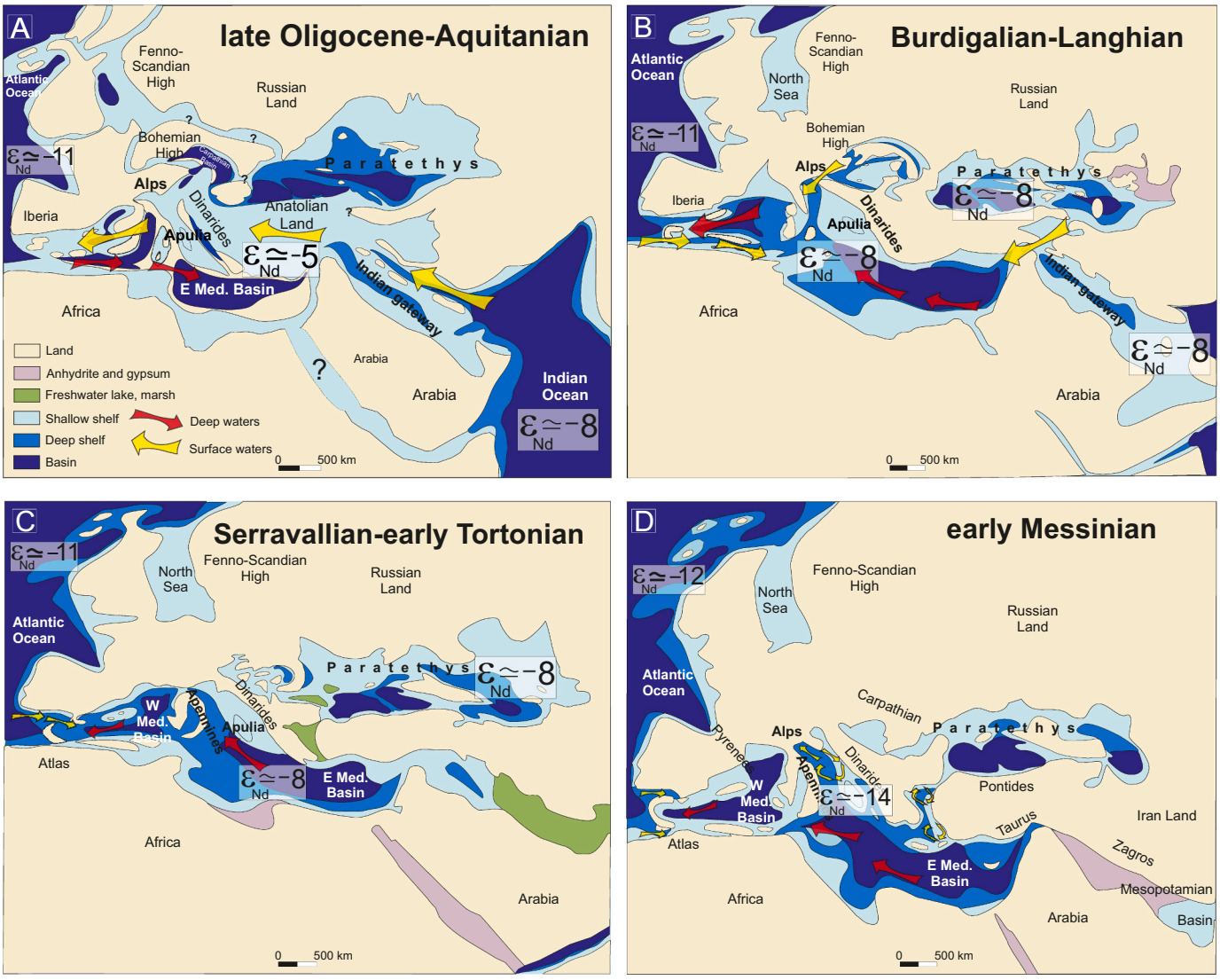

Fig. 3. Simplified paleogeographic maps of the Mediterranean and Paratethys (modified and redrawn from Popov et al., 2004) showing the simplified circulation patterns of the Mediterranean basin and the average Nd isotope signatures of the Mediterranean and the Paratethys and the adjacent oceans. Nd isotope values of the Indian and Atlantic oceans are from O'nions et al. (1998). The paratethys Nd isotope signature is from Kocsis et al. (2009). The Mediterranean Nd isotope signature is the average of the different literature data of Kocsis et al. (2008), Cornacchia et al. (2018), Bialik et al. (2019). A) Paleogeographic map of the Chattian-Aquitanian. B) Paleogographic map of the late Burdigalian-Langhian. C) Paleogeographic map of the Serravallian-Tortonian interval. D) Paleogographic map of the early Messinian.

dataset reported by Kocsis et al. (2008), who analysed the Sr isotope record of different Mediterranean and sub-Alpine hemipelagic successions (Fig. 4A). On the contrary, a datum of the late Aquitanian reported in Cornacchia et al. (2018) shows a deviation of the Sr isotope record of the Central Mediterranean with respect to the global ocean. This deviation is contemporary with the Mi-1a glaciation pulse (Miller et al., 1991; Pekar and DeConto, 2006). The sea-level fall, linked to the glacial maximum, might have reduced water exchanges with adjacent oceans as well as increased weathering of crystalline rocks of the Alpine domain affecting the Central Mediterranean Sr isotope record, which in fact shows a deviation towards heavier values (Fig. 4A, Cornacchia et al., 2018).

In this framework, the Central Mediterranean carbonate platforms (Malta, Latium-Abruzzi, Apula domains) experienced a biocalcification crisis and recorded the Early Miocene Carbon Maximum (EMCM) at the base of the Aquitanian (Fig. 5A, Föllmi et al., 2008; Brandano et al., 2015; Brandano et al., 2017a) when oligophotic facies dominated by LBF are substituted by outer ramp aphotic facies dominated by planktonic foraminifera, sponge spicules and occasionally glauconite. The carbon isotope positive shift, as well as the facies changes, has been attributed to an increased nutrient content of surface waters that led to an excess of primary productivity (Brandano et al., 2015). The high nutrient availability in the Mediterranean waters is testified also by the several phosphatic hardgrounds occurring in the Chattian-Aquitanian hemipelagic successions of Malta and Sicily, linked to increased runoff on a global and regional scale during the Mi-1 Event (John et al., 2003), and formed by deep water currents moving from east to west (Föllmi et al., 2008).

The westward-directed Mediterranean circulation is testified also by the Aquitanian Nd isotope record (Figs. 3A, 4B, Kocsis et al., 2008; Cornacchia et al., 2018). Cornacchia et al. (2018) interpreted this record as evidence of the open connection with the Indian Ocean, which fed the Mediterranean water body (de la Vara et al., 2013; de La Vara and Meijer, 2016). de la Vara et al. (2013) report that the Indian connection was deep enough (1000 m) to let intermediate waters enter in the Mediterranean basin and circulate westward. However, since the signal

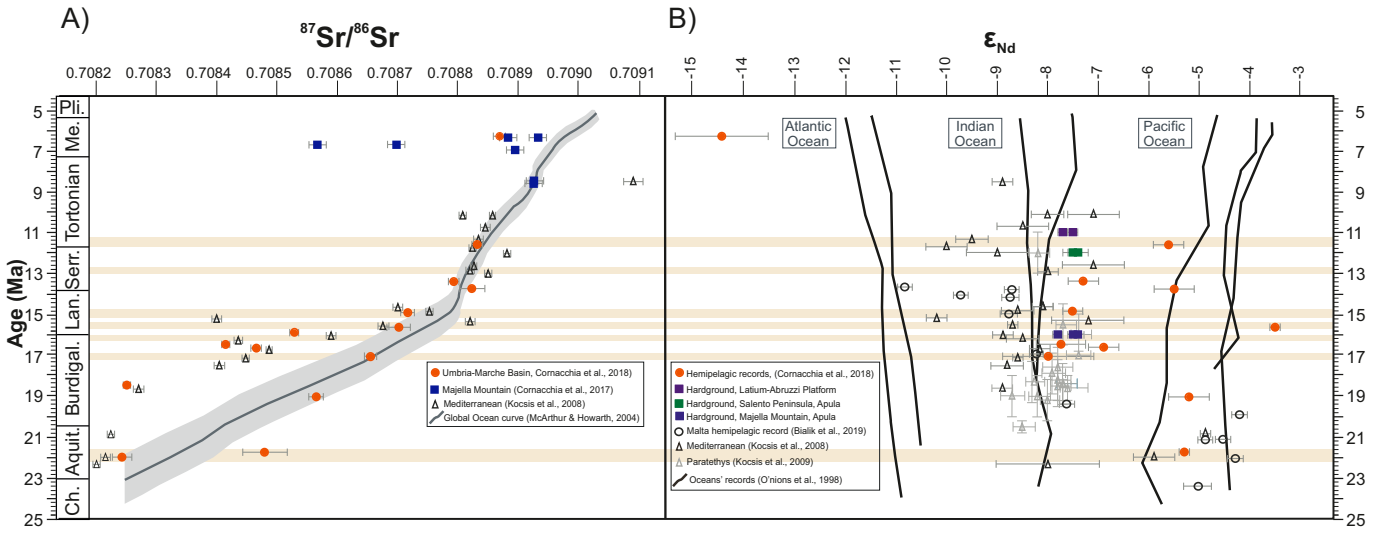

Fig. 4. Compilation of Miocene Sr and Nd isotope records of the Mediterranean area (Modified and redrawn after Cornacchia et al., 2018). A) Compilation of the Sr isotope data from Mediterranean Miocene successions plotted against age. Orange circles refer to mixed planktonic foraminifera of the Umbria-Marche hemipelagic succession (from Cornacchia et al., 2018). Empty triangles refer to mixed fossil assemblages and fish debris from different Mediterranean hemipelagic successions (Kocsis et al., 2008). The blu squares refer to bivalves and brachiopod samples belonging to the Bolognano Fm, cropping out on the Majella Mountain (Cornacchia et al., 2017). The Sr isotope reference line is from McArthur and Howarth (2004). B) Compilation of Nd isotope data from Mediterranean and Paratethyan Miocene successions (in ε notation) plotted against age. Orange circles refer to mixed planktonic foraminifera of the Umbria-Marche hemipelagic succession (from Cornacchia et al., 2018). Empty black triangles refer to mixed fossil assemblages and fish debris from different Mediterranean hemipelagic successions (Kocsis et al., 2008). Light grey triangles refer to fish debris from Paratethys (Kocsis et al., 2009). Empty black circles are from peri-platform material of Malta (Bialik et al., 2019). Blu, green and purple squares refer to shark teeth recovered on phosphatic hardgrounds of Latium-Abruzzi and Apulian Platforms. The reference line for Atlantic, Indian, and Pacific Oceans are from O'nions et al. (1998). Brown-shaded bars represent radiometrically dated volcaniclastic layers interrupting the hemipelagic sedimentation in the Umbria-Marche basin, and attesting the influence of the highly explosive, subduction-related volcanism developed in the Western Mediterranean, in the Central Mediterranean waters as well. The ages of the volcaniclastic levels are from Deino et al. (1997), Mader et al. (2001), Montanari et al. (1997a), and Montanari et al. (1997b).

is not purely Indian but more radiogenic, Cornacchia et al. (2018) state that the intense Eocene-Miocene volcanism of the Iran province (Azizi and Moinevaziri, 2009) affected the Nd isotope signature of the northern Indian Ocean waters entering the Mediterranean. Kocsis et al. (2008) instead, focus their attention mostly on the Western Mediterranean volcanism, which, in their interpretation, lowered the Nd isotope signature of the Mediterranean with respect to the Indian Ocean. Besides the differences in those interpretations, the Sr and Nd isotope records of the Mediterranean basin are in agreement with the main paleogeographic reconstructions (Meulenkamp and Sissingh, 2003; Popov et al., 2004). The Mediterranean basin was indeed a wide and open basin, thus sensitive to global climate changes and carbon cycle perturbations, where the main water mass entered from the Indian Gateway and circulated westward.

In the Burdigalian, the Indo-Pacific connection closed for the first time (Rögl, 1999; Popov et al., 2004; Harzhauser et al., 2007), to open again intermittently several times until the Langhian-Serravallian boundary (Fig. 3B, Popov et al., 2004; Hüsing et al., 2009; Bialik et al., 2019). Along with the first closure of the eastern connection, after the late Burdigalian the circulation of the Mediterranean changed and weakened significantly due to the progressive shallowing of the Indian Gateway (Karami et al., 2009; de la Vara et al., 2013). Karami et al. (2009) stress out the non-linear response of the Mediterranean circulation to this closure in terms of evaporation and sensitivity to fresh-water input. de La Vara and Meijer (2016) propose a box model that shows also the inversion of the Mediterranean-Atlantic circulation, with the onset of short-term antiestuarine circulation patterns with the Atlantic Ocean, depending on the depth of this connection and on atmospheric conditions. The first sapropel levels occur in the Eastern Mediterranean Basin during the middle Miocene, testifying for weaker water exchanges (Rohling et al., 2015). Another hint on the severe control of the Indian connection on the Western Mediterranean is given by Baldassini et al. (2021), who reconstructed the Langhian-Serravallian climatic evolution of the Western Mediterranean through the carbon and oxygen isotope records of planktonic foraminifera of the offshore of the Balearic Islands. The authors say that the Langhian oxygen isotopes record overall testifies for warm waters, which is consistent with the global MMCO. However, they report a strong environmental change at 15.18 Ma, when waters passed from high to low salinity, and more open conditions. This shift was interpreted as due to a short opening phase of the Indian Gateway, which testifies for the strong influence of the Indian Gateway, even on the other side of the Mediterranean basin. Furthermore, from early to middle Miocene, the Paratethys basin was open and connected with the Mediterranean basin (Rögl, 1999; Popov et al., 2004). Then, in the early Serravallian, tectonic changes coupled with the sea-level drop recorded at 13.8 Ma led to the closure of the Mediterranean-Paratethys connection (Simon et al., 2019).

The late Burdigalian-Langhian Sr isotope record of the Central Mediterranean shows an overall deviation from the contemporary global ocean curve (Fig. 4A, Kocsis et al., 2008; Cornacchia et al., 2018). This deviation has been attributed to the highly explosive volcanism developed in the Western Mediterranean (Fig. 1D, E, Lustrino et al., 2009), which affected the seawater chemistry of the Mediterranean water body, especially considering the new, more restricted, paleoceanographic regime. Conversely, the Nd isotope record shows a persistent eastern signature (Figs. 3B, 4B, Kocsis et al., 2008; Cornacchia et al., 2018; Bialik et al., 2019). Different interpretations were given to this Nd isotopic signature. Kocsis et al. (2008) point to the Western Mediterranean volcanism as the major cause to lower the Atlantic signal on Mediterranean Nd isotope record, in agreement with the Sr isotope record. Cornacchia et al. (2018) propose an influence of the Paratethys waters into the Mediterranean. The middle Miocene Paratethys Nd isotope signature, in fact, is undistinguishable from the Indian one (Kocsis et al., 2009), the Central Paratethys showed normal marine conditions and

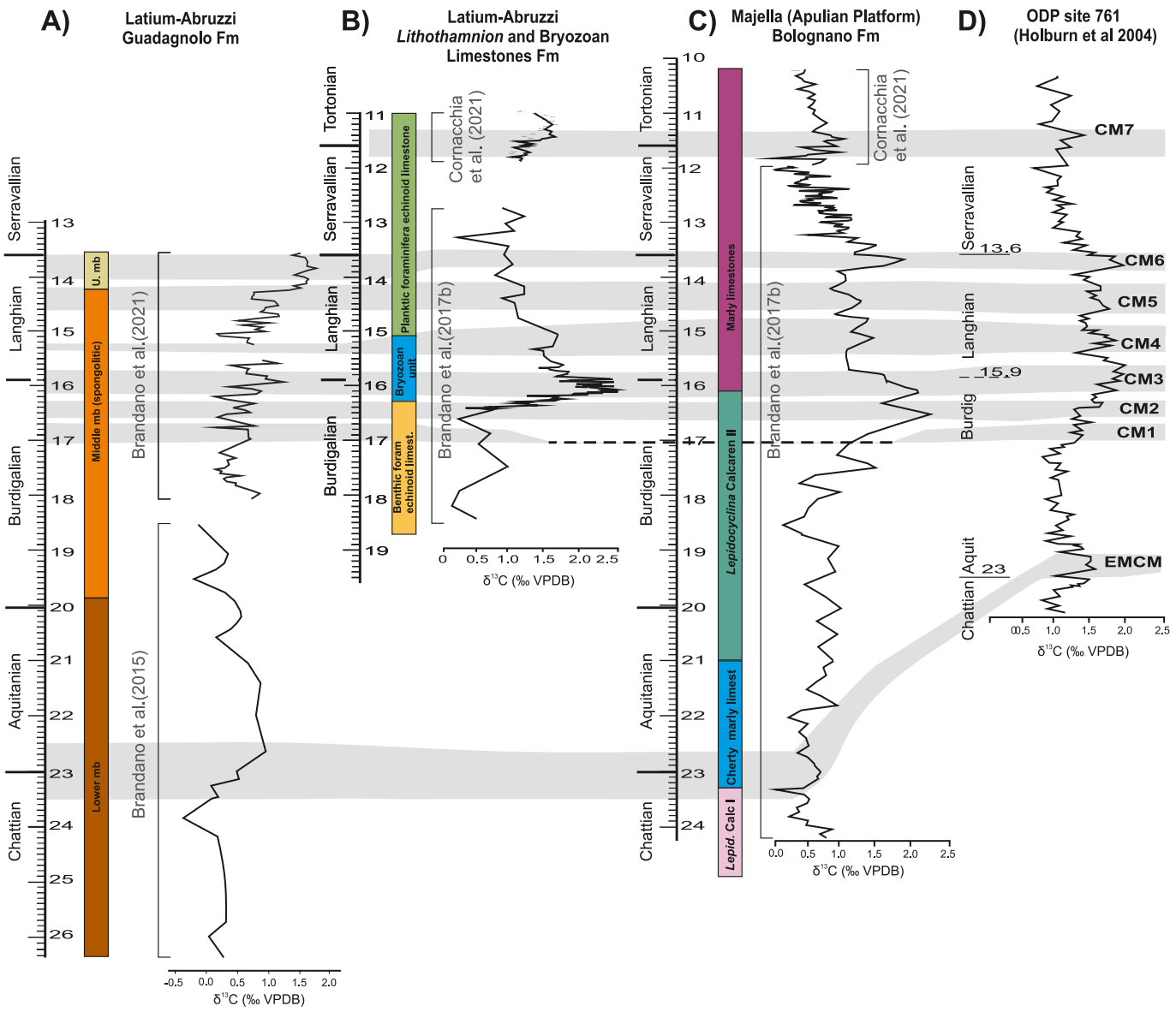

Fig. 5. Correlation of the C-isotope curves of the Latium-Abruzzi and Apulian Platforms with the global Oligo-Miocene C-isotope curve from ODP Site 761 in the Indian Ocean. A) Oligo-Miocene C-isotope record of the Latium-Abruzzi Platform to basin Transition (Guadagnolo Fm, modified and redrawn after Brandano et al., 2015 and 2021). B) Miocene C-isotope curve of the Latium-Abruzzi Platform (modified and redrawn after Brandano et al., 2017b and Cornacchia et al., 2021). C) Oligo-Miocene C-isotope curve of the Majella Mountain (Apulian Platform, modified and redrawn after Brandano et al., 2017b and Cornacchia et al., 2021). D) C-isotope curve of the ODP site 761, located offshore of the southern margin of Australia in the Indian Ocean (modified and redrawn from Holbourn et al., 2004).

was connected to the Central Mediterranean (Simon et al., 2019), and the high sea level sustained by the MMCO should have favoured exchanges between these adjacent basins. Lastly, Bialik et al. (2019), comparing the Central Mediterranean (Malta) Nd isotope record with the Indian Ocean signal (Maldives), imply that the Indian Gateway, besides shallower than in the Aquitanian, could still influence the Mediterranean main water body. Despite these different interpretations, the paleogeographic reconstructions, as well as the Sr and Nd isotope records, point towards a less open Mediterranean, where circulation and hydrodynamic regime weakened significantly. In this newly established paleoceanographic framework, the response of the Mediterranean carbonate systems to the MMCO and Monterey Event is hampered or intensified by regional factors (Fig. 5). This is evident in the carbon isotope record of the Apula and Latium-Abruzzi platforms of the Central Mediterranean, where a carbon isotope excursion twice as wide as the contemporary open ocean record is attested (Fig. 5B, C, Brandano et al., 2017b). The authors state that this carbon isotope excursion was wider than in the global ocean due to regional volcanism as well as by the less efficient circulation after the closure of the Indian Gateway. The fertilizing potential of volcanic ashes on surface waters is well known, since they bring micronutrients, among which Fe, that are necessary to photosynthesis (Duggen et al., 2007, 2010). Simultaneously, an increased CO_2 due to volcanism might have triggered plankton blooms.

However, the Monterey Carbon Isotope Excursion is recorded not only in platform settings, but also in the platform to basin transition in the Latium-Abruzzi Domain (Fig. 5A, Brandano et al., 2021), in the hemipelagic successions of Malta (Jacobs et al., 1996; John et al., 2003), of the Umbria-Marche Basin (Kocsis et al., 2008), as well as on the Balearic Basin, in the Western Mediterranean (Baldassini et al., 2021). In those cases, the carbon isotope excursion is not as wide as in the shallow water record, due to the normal stratification of the water column in terms of C isotope ratios (Jacobs et al., 1996; John et al., 2003; Kocsis et al., 2008), or due to the metabolism of deep benthic components, such as siliceous sponges, that dominated the deep aphotic zone of the

Latium-Abruzzi Domain (Brandano et al., 2021). Furthermore, during the late Burdigalian-Langhian, a second phosphogenic event is recorded in the Eastern and Central Mediterranean, testified by the occurrence of several phosphatic hardgrounds in the Malta and Sicily hemipelagic record (Föllmi et al., 2008), as well as in the northern sector of the Apula Platform (Majella Mountain, Mutti and Bernoulli, 2003; Brandano et al., 2016a). As for the Chattian-Aquitanian interval, these hardgrounds testify for an increased nutrient content of Mediterranean waters related to the global MMCO and Monterey Event (John et al., 2003; Föllmi et al., 2008), and for a westward-directed circulation pattern of deep water currents originating in the Eastern Mediterranean (Mutti and Bernoulli, 2003). In fact, the Nd isotope record of the upper Burdigalian phosphatic hardground cropping out on the Majella Mountain (Fig. 4B) points towards an eastern provenance of these nutrient-rich deep-water currents.

In the Serravallian-Tortonian, the Central Mediterranean Sr isotope record equals the global ocean signal of McArthur and Howarth (2004), testifying for a well-connected main Mediterranean water body, not affected by significant regional volcanism nor weathering (Fig. 4A; Kocsis et al., 2008; Cornacchia et al., 2018). In the same interval though, the Eastern Mediterranean started suffering incipient restricted circulation and several sub-basins in Turkey show a Sr isotope record lower than the global Ocean starting from 8.5 Ma (Schildgen et al., 2014). The deviation of the local Sr isotope record is attributed to local uplift and consequent development of small basins (Cosentino et al., 2012), restricted even in comparison to the main central Mediterranean water body. In this context, the riverine input, enhanced by humid climate conditions (Böhme et al., 2008), influenced the newly formed eastern sub-basins, which show significant differences among them in terms of Sr isotope signature even if closely spaced (Schildgen et al., 2014). These results agree with the previous study of Flecker and Ellam (2006), who stated that in the Tortonian the amount of Atlantic waters entering in the Turkish sub-basins dropped to 50% with respect to middle Miocene.

The Nd isotope record of the same interval is more puzzling, since it still shows a signature similar to the Paratethys and Indian Ocean, when the only ocean in connection with the Mediterranean was the Atlantic (Figs. 3C, 4B, Kocsis et al., 2008; Cornacchia et al., 2018). Cornacchia et al. (2018), analysing the record of the Umbria-Marche basin, hypothesized a persistent influence of the Paratethys water body, which shows the same Nd isotope signal (Kocsis et al., 2009). Kocsis et al. (2008) stress out the fact that the Paratethyan influence must have been intermittent in this phase, mostly controlled by local tectonics, and state that the Nd values between ε_{Nd} −7 and ε_{Nd} −9 testify for locally evolved waters within the Mediterranean basin, thus influenced by weathering of local lithologies. Karami et al. (2009), modelling the consequences of the Indian Gateway closure in the Serravallian, state that, in the post-closure period, the evaporation exceeded the freshwater input, leading to a longer residence time of Mediterranean waters into the basin. Lastly, de La Vara and Meijer (2016) stress out that the closure of the Indian Gateway affected in non-linear ways the overall Mediterranean circulation, potentially weakening also the exchanges with the Atlantic Ocean. The hypothesis of a newly established Mediterranean Nd isotope signature in the middle to late Miocene is supported also by the comparison with the Present. Nowadays, Mediterranean waters show an average ε_{Nd} of −10, −9, which places them in between the pure Atlantic and the pure Indian signals (Spivack and Wasserburg, 1988). Furthermore, Wu et al. (2019) show how the deep waters of the Eastern Mediterranean are nowadays significantly more radiogenic than the main Mediterranean water body (ε_{Nd} of −6, −5). Therefore, it is possible that also in the middle to late Miocene, characterized by a warm and humid climate, regional riverine input controlled the Nd isotope signature of Eastern Mediterranean, and then these eastern waters moved towards the central portion of the basin. In fact, Nd isotopes measured on selected shark teeth recovered from hardground surfaces on the Apulian Platform (Salento Peninsula, Southern Italy) and Latium-Abruzzi Platform (Central Apennines), show Nd isotope ratios between ε_{Nd} −8 and −7 (Fig. 4B). This latter hardground testifies the third phosphogenetic event of the Mediterranean during Miocene. Tortonian phosphatic hardgrounds occur in Malta and Sicily (Föllmi et al., 2008), in the Latium-Abruzzi Platform (Brandano et al., 2020), but also in the Western Mediterranean in the Menorca Island record (Brandano et al., 2016b). Overall, they have been linked to an increased runoff sustained by humid climate (Brandano et al., 2016b), but also to a global intensification of ocean circulation, which led to a global carbon maximum named CM7 (Holbourn et al., 2004), that was identified also in different Mediterranean records (John et al., 2003; Cornacchia et al., 2021, Fig. 5B, C).

During the Messinian, the complex geodynamic evolution of the Mediterranean area led to the development of marginal basins in the Eastern (offshore Cyprus, Gennari et al., 2018) and in the Central Mediterranean, such as the proto-Adriatic basin (Cornacchia et al., 2017). Furthermore, an overall further restriction of the basin occurred due to the progressive narrowing of the Betic corridor, which closed in the late Messinian leading to the complete isolation of the Mediterranean and the onset of the salinity crisis (Martín et al., 2009; Dela Pierre et al., 2011; Manzi et al., 2013).

Prior to the onset of the Messinian Salinity Crisis, the Sr isotope record of marginal sub-basins in the Eastern and Central Mediterannean deviated from the global ocean record towards lighter values, despite the absence of significant volcanism in the area (Schildgen et al., 2014; Cornacchia et al., 2017, 2018; Gennari et al., 2018). This deviation is due to the onset of restricted circultation patterns that led riverine input exercise a major control on local seawater chemistry (Gennari et al., 2018). Furthermore, the local tectonic evolution of the Apennines in the Central Mediterranean defined its paleogeography and favoured the increase of local runoff. This is best shown by the proto-Adriatic basin, that achieved its present form of a narrow, shallow basin already by the early Messinian (Fig. 3D). In this framework, Cornacchia et al. (2017) state that the Sr isotope record deviates towards lighter values since the most common outcropping lithologies are Mesozoic limestones, involved in the Apennine orogenesis, and characterized by lower Sr isotopes values than Miocene waters (Fig. 4A). Lastly, the Nd isotope record of the proto-Adriatic differs completely from the previous intervals, being close but not coincident with the Atlantic signature (Figs. 3D, 4B). The similarity of the records shows that the oceanic inflow in the Messinian came from the western connection. However, the difference between the Atlantic and the proto-Adriatic Nd isotope values is a further evidence of restricted water exchanges between the main Mediterranean water body and the proto-Adriatic waters (Cornacchia et al., 2018).

5. Mediterranean carbonate production trends during Miocene

The classical depositional model for Oligo-Miocene carbonate platforms of the Mediterranean area is the original model of Buxton and Pedley (1989), mutuated from the Chattian carbonate succession of Malta. In the past years, the classical model of Buxton and Pedley (1989) has been modified to describe the different Mediterranean ramps during Oligo-Miocene, which evolved following the evolutionary trends of carbonate producers and controlled by global and regional causes that determined environmental changes (Pomar et al., 2004; Pomar et al., 2012; Brandano et al., 2017a; Coletti et al., 2019).

The authors identify an inner ramp, developed within the euphotic zone, where a grainstone barrier separates the peritidal and lagoonal facies from seagrass meadows that thrived towards the deeper portions of the ramp. In the middle, oligophotic ramp, the carbonate production is dominated by red algae in the upper portion and Larger Benthic Foraminifera (LBF) in the deeper oligophotic zone. Coral patch reefs developed in the Chattian to early Miocene ramps in the mesophotic middle ramp together with red algae (Pomar and Hallock, 2007; Pomar et al., 2014; Pomar et al., 2017). In the outer ramp, developed in the aphotic zone, the LBF associations are substituted by a photo-independent carbonate production dominated by molluscs, small

benthic foraminifera and planktonic foraminifera, whose abundance increases towards the basin (Buxton and Pedley, 1989).

In the early Miocene, before the first closure of the Indian Gateway, the Mediterranean carbonate production is dominated by LBF, which thrived in the oligophotic middle ramp, in oligotrophic conditions and usually under the action of strong currents favoured by the efficient circulation of the basin (Pomar et al., 2017, Fig. 6). In the euphotic zone, seagrass meadows hosted an epiphytic carbonate production dominated by *foralgal -sensu* Wilson and Vecsei (2005)- skeletal assemblage (Brandano et al., 2019, Fig. 6). This is attested in the Central Mediterranean platforms, such as the Latium-Abruzzi (Brandano et al., 2017a) and Apula Platforms (Brandano et al., 2012, 2016a). Coral fragments are present within the LBF-dominated facies of the Eratosthenes Seamount (Coletti et al., 2019), while they form small mounds in the early Miocene record of southern Turkey, where they grow together with red algae in mixed carbonate-siliciclastic systems, strongly controlled by local tectonics (Bassant et al., 2005). In the Central Mediterranean, coral mounds occur in the Aquitanian record of the Pelagian Domain (Sicily, Pedley, 1996) as well as in mixed carbonate-siliciclastic facies of the Burdigalian of Northern Sardinia (Benisek et al., 2009, 2010; Brandano et al., 2010). Conversely, in the Latium-Abruzzi platform, a small *Porites* coral carpet occurs in the Burdigalian within the mesophotic zone, where it interfingers with the seagrass facies (Brandano, 2003). In this case, local paleoceanographic and trophic conditions led to the development of a narrow euphotic zone, which passes rapidly towards a middle ramp dominated by rhodoliths and bryozoans (Brandano and Corda, 2002). Larger coral bioconstructions developed in the meso- and oligophotic zone of mixed carbonate siliclastic shelf in the South Corsica (Tomassetti et al., 2013; Tomassetti and Brandano, 2013; Galloni et al., 2014; Brandano et al., 2016d). Coral buildups and coral carpets are also abundant in the oligophotic zone of the Zincir Kaya platform (Mut Basin) and of the Ermenek Platform outcropping in the South Turkey (Bassant et al., 2005; Janson et al., 2007; Pomar et al., 2012; Vescogni et al., 2014).

From the late Burdigalian, the Mediterranean ramps experienced a deterioration of trophic conditions that produced an expansion of the oligophotic and aphotic carbonate factories (Brandano et al., 2017a; Pomar et al., 2017). Red algae increase globally in the meso- and oligophotic zone, favoured by the MMCO and the increased nutrient content of waters linked to the Monterey Event (Halfar and Mutti, 2005; Fig. 6). Red algae-dominated facies developed from the late Burdigalian to the Tortonian in the Mediterranean area as well (Pomar et al., 2017). Rhodoliths are attested in the middle Miocene record of the Eastern Mediterranean (Bassant et al., 2005; Coletti et al., 2019, Coletti and Basso, 2020), as well as in the middle ramp of the Latium-Abruzzi platform in the Central Mediterranean (Brandano et al., 2017a and references therein). Red algae are a wide group adapted to live at all latitudes and in different light and energy conditions. Therefore, they did not suffer the same crisis as LBF did after the closure of the Indian Gateway and the major change in Mediterranean paleoceanography, but instead occupied that portion of the mesophotic middle ramp that was previously dominated by LBFs. Furthermore, being able of making photosynthesis up the 4% of light that impacts the sea-surface, they were not particularly sensitive to the increased turbidity related to the Monterey Event, but might as well be favoured by the nutrient availability. Pomar et al. (2017), in fact, says that the Cenozoic Tethys trend of abundance and diversity of red algae parallels the $\delta^{13}C$ curve. Since late Burdigalian, the lower oligophotic and aphotic zones of Mediterranean ramps are characterized by the spread of bryozoan-dominated facies (Carannante et al., 1988; Carannante and Simone, 1996; Bassi et al., 2006; Ruchonnet and Kindler, 2010; Tomassetti et al., 2013; Brandano and Ronca, 2014; Fontana et al., 2015; Salocchi et al., 2018; Fig. 6). The abundance of bryozoans is linked to the increased nutrient availability, and consequent primary productivity, of surface waters, sustained by the MMCO and Monterey Event, but enhanced by regional factors, such as Western Mediterranean volcanism and paleoceanographic conditions (Brandano et al., 2017b). During Langhian to Serravallian, seagrass environments, dominated by a foralgal association, locally expanded. In the Mut and Ermenek regions, small, flat-topped platform developed thanks to a great accumulation of epiphytic biota (Bassant et al., 2005; Janson et al., 2007; Pomar et al., 2012). Coral bioconstructions, largely made of branching and spherical corals encrusted by red algae, are abundant in the platform top and margins. Expansion of seagrass persisted during the late Serravallian, when a cooling phase following the MMCO started, foralgal association accumulated in the seagrass environments and rhodalgal in the mesophotic and oligophotic zone of the Ragusa platform (Fig. 6; Ruchonnet, 2006).

In the early Tortonian, after the MMCO and the carbon cycle perturbation of the Monterey Event, red algae still dominated the meso- and oligophotic zones of Mediterreanean carbonate ramps, while

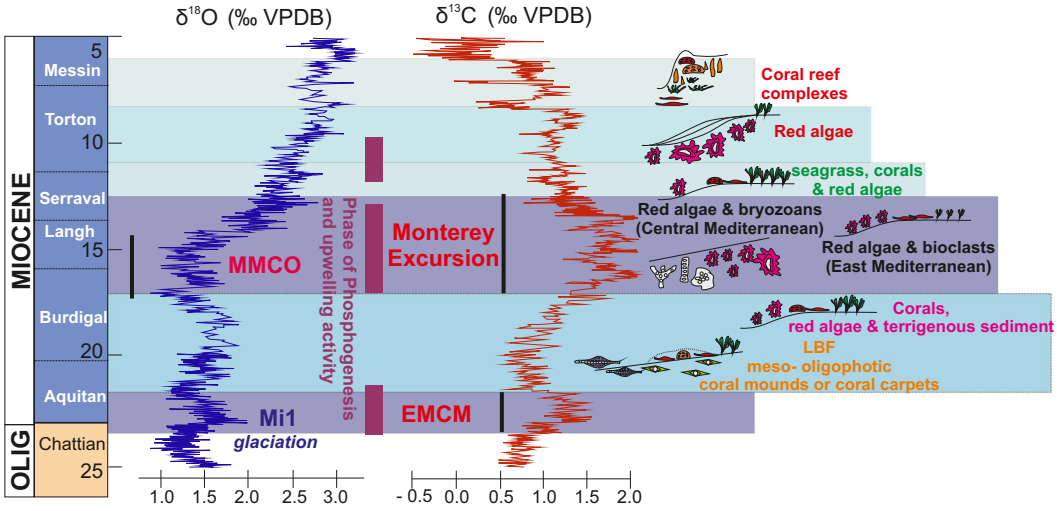

Fig. 6. Miocene climatic events, phases of phosphogenesis and upwelling, oxygen and carbon isotope curves, main Miocene carbonate producers of the Mediterranean area together with their relative ramp and/or platform geometry. Modified and redrawn after Brandano et al. (2019). Aphotic (bryozoan-dominated) and oligophotic (red algae-dominated) carbonate factory expansion coincides with the Monterey Excursion. Seagrass (euphotic) spreading follows the Monterey and the MMCO, but red algae are still dominant carbonate sediment producers. Carbon and oxygen isotope curves are from Cramer et al. (2009) for the Oligocene-Aquitanian and from Zachos et al. (2001) for the Burdigalian-Messinian. EMCM = Early Miocene Carbon Maximum; MMCO = Middle Miocene Climatic Optimum.

seagrass persisted in the euphotic zone (Fig. 6; Mateu-Vicens et al., 2008; Ruchonnet and Kindler, 2010; Pomar et al., 2012, 2017; Brandano et al., 2016c; Coletti and Basso, 2020). In the Ragusa ramp, sediment production in the euphotic zone changed to chlorozoan, although foramol sediments were still present (Ruchonnet, 2006). In the Western Mediterranean, inherited topography and local tectonics led either to the development of high-angle distally steepened ramps, where the slope was formed by clinobeds composed mostly of gravelly-sized rhodoliths (Pomar, 2001b, Pomar et al., 2002; Brandano et al., 2005; Mateu-Vicens et al., 2008), or to homoclinal ramps where red algae occurred together with bryozoans and molluscs (Martín et al., 1996, Fig. 6).

From the late Tortonian to the early Messinian the global climate became progressively cooler and more arid, favouring the establishment of persistent oligotrophic conditions of seawaters (Zachos et al., 2001). This global change is recorded in the Mediterranean with a major carbonate production change: coral build-ups started developing in the shallowest portion of the water column, forming reef complexes (Figs. 6, 7, Esteban, 1996; Kiessling et al., 1999; Pomar et al., 2017 and references therein).

Notwithstanding the fact that the upper Tortonian-lower Messinian coral buildups are characterized by a decrease of generic richness with respect the Oligocene and lower Miocene counterpart (Perrin and Bosellini, 2013), during the transition between early and late Tortonian, zooxanthellate corals became the main reef builders all over the Mediterranean area (Pomar and Hallock, 2007; Pomar et al., 2017).

The best examples of upper Miocene reef complexes occurred in the Western Mediterranean (Fig. 7), testified by the development of rimmed platforms and fringing reefs in southeastern Spain (Braga et al., 1990; Braga and Martín, 1996; Braga et al., 2006), in the Balearic Islands (Pomar, 1991, 2001a, 2001b; Pomar et al., 1996), as well as in the Rif and Tell provinces of Morocco (Esteban et al., 1996). Small coral buildups, however, occur also in the Central Mediterranean in the northern Thyrrenian Sea (Tuscany, Bossio et al., 1996) and southern Thyrrenian Sea (Calabria) as well as in Sicily and Malta (Pedley, 1996; Bialik et al., 2021), in the southernmost portion of the Apula Platform in the Salento area (Bosellini, 2006; Fig. 7), and in the Eastern Mediterranean in the island of Crete (Brachert et al., 2006). In those cases, they do not develop as much to form rimmed platforms, but fringing reefs or small mounds, always in the shallowest portion of the euphotic zone. Conversely, the

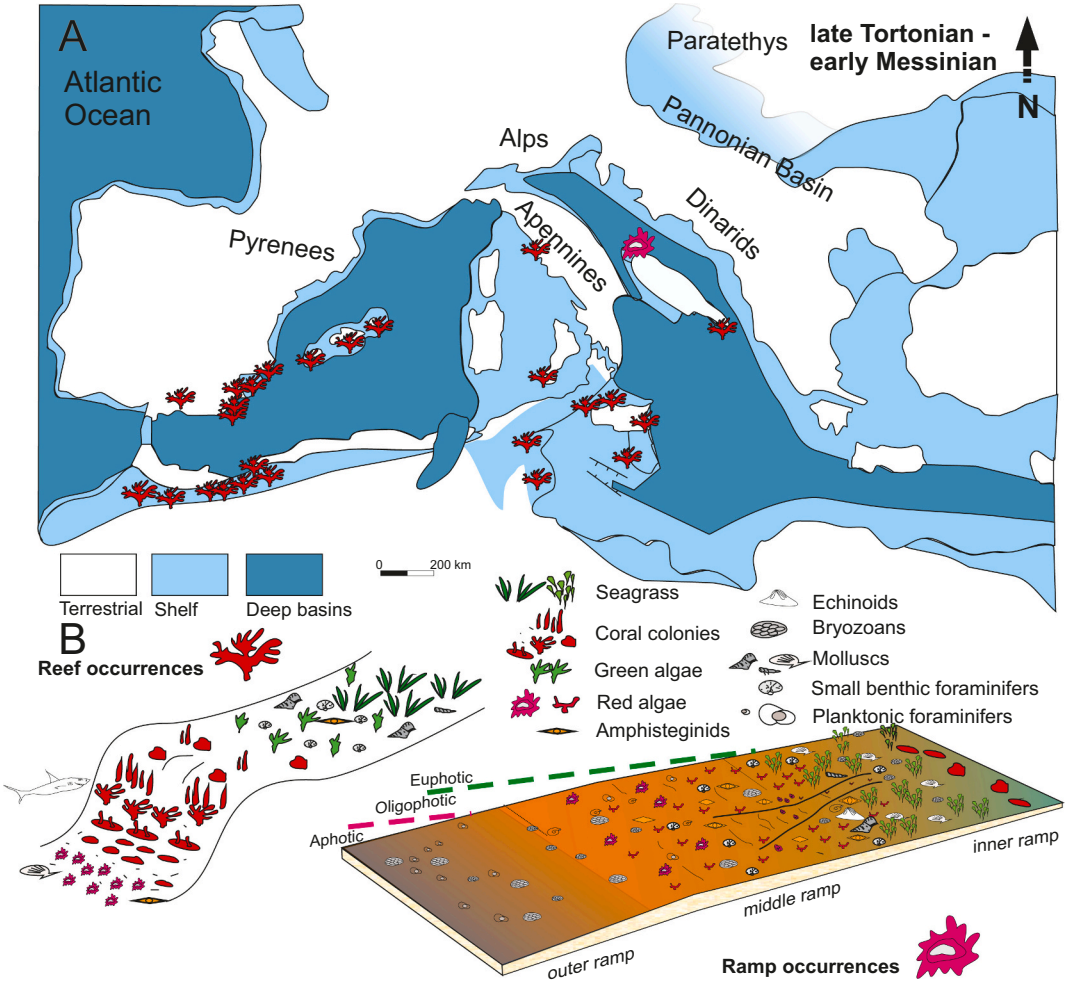

Fig. 7. (A) Paleogeographic map of the Mediterranean area during the late Tortonian – early Messinian showing the occurrences of the upper Miocene reef complexes and the *Lithothamnion* Limestones ramp in the Apulian domain. The paleogeographic map is modified and redrawn after Carminati et al. (2010). The occurrences of reef complexes in the southeastern Spain are from Braga et al. (1990), Braga and Martín et al. (1996); Esteban et al. (1996); in the Balearic Islands from Pomar et al. (1996); in the Rif and Tell provinces of Morocco from Esteban et al. (1996). Central Mediterranean reef occurrences are from Bossio et al. (1996, northern Thyrrenian sea, Tuscany, Italy) and from Pedley, 1996 (Calabria, Sicily and Malta). The occurrence of an upper Miocene reef complex in the Salento Peninsula (Apula Domain, souther Adriatic sea) is from Bosellini (2006). The ramp occurrence in the northern portion of the Apula Domain is attested in Brandano et al. (2016c).
(B) Simplified depositional models of the upper Miocene reef complexes and carbonate ramps showing the differences in the main components and the consequent different geometries of the platforms.

lower Messinian facies of the northernmost portion of the Apula Platform, represented by the Majella Mountain record, located in the proto-Adriatic basin, show a completely different evolution of the ramp (Fig. 7). The upper Tortonian-lower Messinian ramp of the Majella Mountain, in fact, dominated by red algae in the Tortonian, is characterized by a progressive increase of terrigenous input in the lower Messinian as well as the occurrence of small benthic foraminifera (buliminids and bolivinids) resistant to low oxygenated conditions (Brandano et al., 2016c). The authors interpreted this facies change as an evidence of the detrimental trophic conditions of this basin, affected by increased runoff linked to the Apennine orogeny. The different carbonate production in the proto-Adriatic basin compared to coeval Mediterranean carbonate successions is a further evidence of the restricted water circulation established in the early Messinian and testified by the local Sr and Nd isotope record.

To sum up, LBF carbonate production, which dominated in the late Oligocene, persisted in the early Miocene as well (Fig. 6), but was instead significantly affected by the closure of the Indo-Pacific connection in the late Burdigalian. Lepidocyclinds, in fact, disappeared in the Mediterranean basin, while the same group persisted in the Indo-Pacific in the middle Miocene (BouDagher-Fadel, 2008; BouDagher-Fadel, 2018; Wilson and Vecsei, 2005). In the middle Miocene, whit the demise of the LBF, red algae became more important carbonate producers in the meso-oligophotic zone, persisting from the Burdigalian to the Tortonian. Furthermore, the Monterey Event is marked by the spread of bryozoan-dominated facies at greater depths with respect to red algae (Fig. 6).

Lastly, corals occurred throughout the entire Miocene, but in different facies, abundances and geometries in different moments. In the early and middle Miocene, they formed coral carpets or mesophotic mounds (Fig. 6). During this interval, they never represent the main carbonate-producing facies of carbonate ramps, and their occurrence is strictly controlled by local factors. It is indeed in the late Tortonian-early Messinian that coral production shows a major change since they start forming proper reef complexes throughout the entire Mediterranean (Figs. 6, 7), with the exception of restricted sub-basins, where the excess of nutrients and the lack of efficient water circulation inhibited coral production. In these basins, red algae continue to dominate (Brandano et al., 2016c; Cornacchia et al., 2017).

6. Conclusions

The Miocene oceanographic evolution of the Mediterranean area is extremely complex and fascinating, since in this time interval the Mediterranean acquired its actual shape. In this framework, global and local controlling factors on seawater chemistry affected carbonate production also according to the paleoceanographic conditions of the Mediterranean and their changes through time.

Aquitanian Sr and Nd isotope records of the Mediterranean attest an open basin, fed by the Indian Ocean and dominated by an overall westward circulation, sensitive to global climate changes and carbon cycle perturbations. In this context, carbonate ramps are dominated by LBF, while corals occur as mounds in the lowest portion of the middle ramp or as coral carpets, strongly influenced by local conditions.

From the late Burdigalian, the progressive shallowing and intermittent connection with the Indian Ocean changed the overall circulation in the basin, leading to higher residence time of Mediterranean waters and smaller water exchanges not only with the Indian, but also with the Atlantic Ocean. In this newly established paleoceanographic framework, regional factors such as volcanism, were able to affect Central Mediterranean seawater chemistry more than in the previous periods. The Sr isotope record of the Central Mediterranean, in fact, deviates towards lighter values, while Nd isotope record shows active exchanges with the Paratethys, favoured also by the high sea level linked to MMCO. LBF assemblages are the most affected by the Indo-Pacific closure. They show a demise in the Mediterranean basin after the Burdigalian, while persist in the Indian Ocean. With the LBF demise, carbonate ramps start to be dominated by red algae and bryozoans from the middle Miocene to the Tortonian, with corals persisted as small mounds in the eastern Mediterranean. Furthermore, in the middle Miocene a huge spread of bryozoan-dominated facies is attested in the lower portion of the middle ramp and in the outer ramp. The high bryozoan production was triggered by the global Monterey Event, but enhanced by the regional volcanism and paleoceanographic conditions.

From the Tortonian to the Messinian, local tectonics in the Eastern and Central Mediterranean led to the development of small sub-basins characterized by restricted water exchanges with the main Mediterranean water body, as attested by the deviation of Sr isotope records of the Eastern sub-basins in the Tortonian, and of the proto-Adriatic basin in the lower Messinian. In the early Messinian, corals started to form proper reef complexes and fringing reefs in the Western and Central Mediterranean, with the exception of the small restricted sub-basins, such as the proto-Adriatic basin, where red algae and small benthic foraminifera persisted.

Therefore, this review shows how carbonate production trends and changes, overall controlled by evolutionary trends and global climate, were extremely affected also by the paleocenographic evolution of the Mediterranean area.

Declaration of Competing Interest

The authors declare that they have no known competing financial interests or personal relationships that could have appeared to influence the work reported in this paper.

Acknowledgments

This study has been supported by IGG-CNR-P0CT0061 funds to S. Agostini. Laura Tomassetti is sincerely thanked for the helpful discussions on carbonate production and carbonate facies changes. Editor Alessandra Negri and reviewers Daniela Basso and Nereo Preto are sincerely thanked for their comments and criticisms which significantly improved the manuscript.

References

Agostini, S., Doglioni, C., Innocenti, F., Manetti, P., Tonarini, S., 2010. On the geodynamics of the Aegean rift. Tectonophysics 488 (1–4), 7–21.

Azizi, H., Moinevaziri, H., 2009. Review of the tectonic setting of Cretaceous to Quaternary volcanism in northwestern Iran. J. Geodyn. 47, 167–179.

Baldassini, N., Foresi, L.M., Lirer, F., Sprovieri, M., Turco, E., Pelosi, N., Di Stefano, A., 2021. Middle Miocene stepwise climate evolution in the Mediterranean region through high-resolution stable isotopes and calcareous plankton records. Mar. Micropaleontol. 102030.

Bassant, P., Van Buchem, F.S.P., Strasser, A., Görür, N., 2005. The stratigraphic architecture and evolution of the Burdigalian carbonate—siliciclastic sedimentary systems of the Mut Basin, Turkey. Sediment. Geol. 173 (1–4), 187–232.

Bassi, D., Carannante, G., Murru, M., Simone, L., Toscano, F., 2006. Rhodalgal/bryomol assemblages in temperate-type carbonate, channelized depositional systems: the Early Miocene of the Sarcidano area (Sardinia, Italy). Geological Society, London, Special Publications 255, 35–52.

Batenburg, S.J., Voigt, S., Friedrich, O., Osborne, A.H., Bornemann, A., Klein, T., Pérez Dìaz, L., Frank, M., 2018. Major intensification of Atlantic overturning circulation at the onset of Paleogene greenhouse warmth. Nat. Commun. 9 (1), 1–8.

Benisek, M.F., Betzler, C., Marcano, G., Mutti, M., 2009. Coralline-algal assemblages of a Burdigalian platform slope: implications for carbonate platform reconstruction (northern Sardinia, western Mediterranean Sea). Facies 55 (3), 375–386.

Benisek, M.F., Marcano, G., Betzler, C., 2010. Facies and stratigraphic architecture of a Miocene warm-temperate to tropical fault-block carbonate platform, Sardinia. Int. Assoc. Sedimentol. Spec. Publ. 42, 129–148.

Bertram, C.J., Elderfield, H., 1993. The geochemical balance of the rare earth elements and neodymium isotopes in the oceans. Geochim. Cosmochim. Acta 57 (9), 1957–1986.

Bialik, O.M., Frank, M., Betzler, C., Zammit, R., Waldmann, N.D., 2019. Two-step closure of the Miocene Indian Ocean Gateway to the Mediterranean. Sci. Rep. 9 (1), 1–10.

Bialik, O.M., Zammit, R., Micallef, A., 2021. Architecture and sequence stratigraphy of the Upper Coralline Limestone formation, Malta–implications for Eastern Mediterranean restriction prior to the Messinian Salinity Crisis. Deposit. Rec. 1–15. https://doi.org/10.1002/dep2.138.

Böhme, M., Ilg, A., Winklhofer, M., 2008. Late Miocene "washhouse" climate in Europe. Earth Planet. Sci. Lett. 275 (3–4), 393–401.
Bosellini, F.R., 2006. Biotic changes and their control on Oligocene-Miocene reefs: a case study from the Apulia Platform margin (southern Italy). Palaeogeogr. Palaeoclimatol. Palaeoecol. 241 (3–4), 393–409.
Bossio, A., Esteban, M., Mazzanti, R., Mazzei, R., Salvatorini, G., 1996. Rosignano reef complex (Messinian), Livornesi Mountains, Tuscany, Central Italy. In: Franseen, E.K., Esteban, M., Ward, W., Rouchy, J. (Eds.), Models for Carbonate Stratigraphy from Miocene Reef Complexes of Mediterranean Regions, vol. 5. SEPM Concepts in Sedimentology and Paleontology, Tulsa, pp. 277–294.
BouDagher-Fadel, M.K., 2008. Biology and evolutionary history of larger benthic foraminifera. Dev. Palaeontol. Stratigr. 21, 1–37.
BouDagher-Fadel, M.K., 2018. Evolution and Geological Significance of Larger Benthic Foraminifera. University College London Press, London.
Brachert, T.C., Reuter, M., Felis, T., Kroeger, K.F., Lohmann, G., Micheels, A., Fassoulas, C., 2006. Porites corals from Crete (Greece) open a window into Late Miocene (10 Ma) seasonal and interannual climate variability. Earth Planet. Sci. Lett. 245 (1–2), 81–94.
Braga, J.C., Martín, J.M., 1996. Geometries of reef advance in response to relative sea-level changes in a Messinian (uppermost Miocene) fringing reef (Cariatiz reef, Sorbas Basin, SE Spain). Sediment. Geol. 107 (1–2), 61–81.
Braga, J.C., Martín, J.M., Alcala, B., 1990. Coral reefs in coarse-terrigenous sedimentary environments (Upper Tortonian, Granada Basin, southern Spain). Sediment. Geol. 66 (1–2), 135–150.
Braga, J.C., Martin, J.M., Beztler, C., Aguirre, J., 2006. Models of temperate carbonate deposition in Neogene basins in SE Spain: a synthesis. In: Pedley, H.M., Carannante, G. (Eds.), Cool Water Carbonates: Depositional Systems and Paleoenvironmental Controls, vol. 255. Soc. London Spec. Publ, Geol, p. 121e135.
Brandano, M., 2003. Tropical/subtropical inner ramp facies in lower Miocene 'Calcari a Briozoi e Litotamni' of the Monte Lungo area (Cassino plain, Central Apennines, Italy). Boll. Soc. Geol. Ital. 122, 85–98.
Brandano, M., Corda, L., 2002. Nutrients, sea level and tectonics: constrains for the facies architecture of a Miocene carbonate ramp in central Italy. Terra Nova 14 (4), 257–262.
Brandano, M., Ronca, S., 2014. Depositional processes of the mixed carbonate–siliciclastic rhodolith beds of the Miocene Saint-Florent Basin, northern Corsica. Facies 60 (1), 73–90.
Brandano, M., Vannucci, G., Pomar, L., Obrador, A., 2005. Rhodolith assemblages from the lower Tortonian carbonate ramp of Menorca (Spain): environmental and paleoclimatic implications. Palaeogeogr. Palaeoclimatol. Palaeoecol. 226 (3–4), 307–323.
Brandano, M., Tomassetti, L., Bosellini, F., Mazzucchi, A., 2010. Depositional model and paleodepth reconstruction of a coral-rich, mixed siliciclastic-carbonate system: the Burdigalian of Capo Testa (northern Sardinia, Italy). Facies 56 (3), 433–444.
Brandano, M., Lipparini, L., Campagnoni, V., Tomassetti, L., 2012. Downslope-migrating large dunes in the Chattian carbonate ramp of the Majella Mountains (Central Apennines, Italy). Sediment. Geol. 255, 29–41.
Brandano, M., Lustrino, M., Cornacchia, I., Sprovieri, M., 2015. Global and regional factors responsible for the drowning of the Central Apennine Chattian carbonate platforms. Geol. J. 50 (5), 575–591.
Brandano, M., Cornacchia, I., Raffi, I., Tomassetti, L., 2016a. The Oligocene–Miocene stratigraphic evolution of the Majella carbonate platform (Central Apennines, Italy). Sediment. Geol. 333, 1–14.
Brandano, M., Westphal, H., Mateu-Vicens, G., Preto, N., Obrador, A., 2016b. Ancient upwelling record in a phosphate hardground (Tortonian of Menorca, Balearic Islands, Spain). Mar. Pet. Geol. 78, 593–605.
Brandano, M., Tomassetti, L., Sardella, R., Tinelli, C., 2016c. Progressive deterioration of trophic conditions in a carbonate ramp environment: the Lithothamnion Limestone, Majella Mountain (Tortonian–early Messinian, central Apennines, Italy). Palaios 31 (4), 125–140.
Brandano, M., Bosellini, F., Mazzucchi, A., Tomassetti, L., 2016d. Coral assemblages and bioconstructions adapted to the depositional dynamics of a mixed carbonate-siliciclastic setting: the case study of the Burdigalian Bonifacio Basin (South Corsica). Riv. Ital. Paleontol. Stratigr. 122 (1), 37–52.
Brandano, M., Cornacchia, I., Tomassetti, L., 2017a. Global versus regional influence on the carbonate factories of Oligo-Miocene carbonate platforms in the Mediterranean area. Mar. Pet. Geol. 87, 188–202.
Brandano, M., Cornacchia, I., Raffi, I., Tomassetti, L., Agostini, S., 2017b. The Monterey Event within the Central Mediterranean area: The shallow-water record. Sedimentology 64 (1), 286–310.
Brandano, M., Tomassetti, L., Mateu-Vicens, G., Gaglianone, G., 2019. The seagrass skeletal assemblage from modern to fossil and from tropical to temperate: Insight from Maldivian and Mediterranean examples. Sedimentology 66 (6), 2268–2296.
Brandano, M., Ronca, S., Di Bella, L., 2020. Erosion of Tortonian phosphatic intervals in upwelling zones: The role of internal waves. Palaeogeogr. Palaeoclimatol. Palaeoecol. 537, 109405.
Brandano, M., Cornacchia, I., Catanzariti, R., Tomassetti, L., 2021. The Monterey Event in the Mediterranean platform to basin transition: the Guadagnolo Formation (Miocene, Prenestini Mountains, Central Apennines). Palaeogeogr. Palaeoclimatol. Palaeoecol. 564 (110177), 1–13.
Buxton, M.W.N., Pedley, H.M., 1989. Short Paper: a standardized model for Tethyan Tertiary carbonate ramps. J. Geol. Soc. 146 (5), 746–748.
Cao, W., Zahirovic, S., Flament, N., Williams, S., Golonka, J., Müller, R.D., 2017. Improving global paleogeography since the late Paleozoic using paleobiology. Biogeosciences 14 (23), 5425–5439.
Carannante, G., Esteban, M., Milliman, J.D., Simone, L., 1988. Carbonate lithofacies as paleolatitude indicators: problems and limitations. Sediment. Geol. 60 (1–4), 333–346.
Carannante, G., Simone, L., 1996. Rhodolith facies in the central-southern Apennines mountains, Italy. In: Models for Carbonate Stratigraphy from Miocene Reef Complexes of Mediterranean Regions (Eds E.K. Franseen, M. Esteban,W. Ward and J. Rouchy), SEPM Concepts Sedimentol. Paleontol. 5, 261–275.
Carminati, E., Doglioni, C., 2005. Mediterranean tectonics. Encyc. Geol. 2, 135–146.
Carminati, E., Lustrino, M., Cuffaro, M., Doglioni, C., 2010. Tectonics, magmatism and geodynamics of Italy: what we know and what we imagine. J. Virtual Explor. 36 (8), 10–3809.
Carminati, E., Lustrino, M., Doglioni, C., 2012. Geodynamic evolution of the central and western Mediterranean: Tectonics vs. igneous petrology constraints. Tectonophysics 579, 173–192.
Coletti, G., Basso, D., 2020. Coralline algae as depth indicators in the Miocene carbonates of the Eratosthenes Seamount (ODP Leg 160, Hole 966F). Geobios 60, 29–46.
Coletti, G., Basso, D., Betzler, C., Robertson, A.H., Bosio, G., El Kateb, A., Foubert, A., Meilijson, A., Spezzaferri, S., 2019. Environmental evolution and geological significance of the Miocene carbonates of the Eratosthenes Seamount (ODP Leg 160). Palaeogeogr. Palaeoclimatol. Palaeoecol. 530, 217–235.
Cornacchia, I., Andersson, P., Agostini, S., Brandano, M., Di Bella, L., 2017. Strontium stratigraphy of the upper Miocene Lithothamnion Limestone in the Majella Mountain, central Italy, and its palaeoenvironmental implications. Lethaia 50 (4), 561–575.
Cornacchia, I., Agostini, S., Brandano, M., 2018. Miocene oceanographic evolution based on the Sr and Nd isotope record of the Central Mediterranean. Paleoceanogr. Paleoclimatol. 33 (1), 31–47.
Cornacchia, I., Munnecke, A., Brandano, M., 2021. The potential of carbonate ramps to record C-isotope shifts: insights from the upper Miocene of the Central Mediterranean area. Lethaia 54 (1), 73–89.
Cosentino, D., Schildgen, T.F., Cipollari, P., Faranda, C., Gliozzi, E., Hudáčková, N., Lucifora, S., Strecker, M.R., 2012. Late Miocene surface uplift of the southern margin of the Central Anatolian Plateau, Central Taurides, Turkey. Geol. Soc. Am. Bull. 124, 133–145.
Coxall, H.K., Huck, C.E., Huber, M., Lear, C.H., Legarda-Lisarri, A., O'regan, M., Sliwinska, K.K., van de Flierdt, T., de Boer, A.M., Zachos, J.C., Backman, J., 2018. Export of nutrient rich Northern Component Water preceded early Oligocene Antarctic glaciation. Nat. Geosci. 11 (3), 190–196.
Cramer, B.S., Toggweiler, J.R., Wright, J.D., Katz, M.E., Miller, K.G., 2009. Ocean overturning since the Late Cretaceous: Inferences from a new benthic foraminiferal isotope compilation. Paleoceanography 24 (4), PA4216.
De Boer, B., Van de Wal, R.S.W., Bintanja, R., Lourens, L.J., Tuenter, E., 2010. Cenozoic global ice-volume and temperature simulations with 1-D ice-sheet models forced by benthic $\delta^{18}O$ records. Ann. Glaciol. 51, 23–33.
de La Vara, A., Meijer, P., 2016. Response of Mediterranean circulation to Miocene shoaling and closure of the Indian Gateway: a model study. Palaeogeogr. Palaeoclimatol. Palaeoecol. 442, 96–109.
de la Vara, A., Meijer, P.T., Wortel, M.J.R., 2013. Model study of the circulation of the Miocene Mediterranean Sea and Paratethys: closure of the Indian Gateway. Clim. Past Discuss. 9 (4), 4385–4424. https://doi.org/10.5194/cpd-9-4385-2013.
Deino, A., Channell, J., Coccioni, R., De Grandis, G., DePaolo, D.J., Fornaciari, E., Emmanuel, L., Laurenzi, M.A., Montanari, A., Rio, D., Renard, M., 1997. Integrated stratigraphy of the upper Burdigalian-lower Langhian section at Moria (Marche region, Italy). In: Montanari, A., Odin, G.S., Coccioni, R. (Eds.), Miocene stratigraphy: an integrated approach. Elsevier Science B.V, Amsterdam, Netherlands, pp. 315–341.
Dela Pierre, F., Bernardi, E., Cavagna, S., Clari, P., Gennari, R., Irace, A., Lozar, F., Lugli, S., Manzi, V., Natalicchio, M., Roveri, M., Violanti, D., 2011. The record of the Messinian salinity crisis in the Tertiary Piedmont Basin (NW Italy): the Alba section revisited. Palaeogeogr. Palaeoclimatol. Palaeoecol. 310 (3–4), 238–255.
Dera, G., Pucéat, E., Pellenard, P., Neige, P., Delsate, D., Joachimski, M.M., Reisberg, L., Martinez, M., 2009. Water mass exchange and variations in seawater temperature in the NW Tethys during the Early Jurassic: evidence from neodymium and oxygen isotopes of fish teeth and belemnites. Earth Planet. Sci. Lett. 286 (1–2), 198–207.
Doglioni, C., Agostini, S., Crespi, M., Innocenti, F., Manetti, P., Riguzzi, F., Savascin, Y., 2002. On the extension in western Anatolia and the Aegean Sea. J. Virtual Explor. 8, 169–183.
Duggen, S., Croot, P.L., Schacht, U., Hoffmann, L., 2007. Subduction zone volcanic ash can fertilize the surface ocean and stimulate phytoplankton growth: evidence from the biogeochemical experiments and satellite data. Geophys. Res. Lett. 34 https://doi.org/10.1029/2006GL027522.
Duggen, S., Olgun, N., Croot, P.L., Hoffmann, L., Dietze, H., Delmelle, P., Teschner, C., 2010. The role of airborne volcanic ash for the surface ocean biogeochemical iron-cycle: a review. Biogeoscience 7, 827–844.
Esteban, M., 1996. An overview of Miocene reefs from Mediterranean areas: general trends and facies models. In: Franseen, E.K., Esteban, M., Ward, W., Rouchy, J. (Eds.), Models for Carbonate Stratigraphy from Miocene Reef Complexes of Mediterranean Regions, vol. 5. SEPM Concepts in Sedimentology and Paleontology, Tulsa, pp. 3–53.
Esteban, M., Braga, J.C., Martín, J., De Santisteban, C., 1996. Western Mediterranean reef complexes. Sedimentology, 66(4), 1266-1301. In: Franseen, E.K., Esteban, M., Ward, W., Rouchy, J. (Eds.), Models for Carbonate Stratigraphy from Miocene Reef Complexes of Mediterranean Regions, vol. 5. SEPM Concepts in Sedimentology and Paleontology, Tulsa, pp. 55–72.

Flecker, R., Ellam, R.M., 2006. Identifying late Miocene episodes of connection and isolation in the Mediterranean-Paratethyan realm using Sr isotopes. Sediment. Geol. 188–189, 189–203.
Föllmi, K.B., Renevey, J.P., De Kaenel, E., Stilles, P., 2008. Stratigraphy and sedimentology of phosphate-rich sediments in Malta and southeastern Sicily (latest Oligocene to early Late Miocene). Sedimentology 55, 1029–1051.
Fontana, D., Conti, S., Fioroni, C., Grillenzoni, C., 2015. Factors controlling the evolution of a wedge-top temperate-type carbonate platform in the Miocene of the northern Apennines (Italy). Sediment. Geol. 319, 13–23.
Frank, M., 2002. Radiogenic isotopes: Tracers of past ocean circulation and erosional input. Rev. Geophys. 40 (1), 1001. https://doi.org/10.1029/2000RG000094.
Frost, C.D., O'Nions, R.K., Goldstein, S.L., 1986. Mass balance for Nd in the Mediterranean Sea. Chem. Geol. 55, 45–50.
Galloni, F., Chaix, C., Cornée, J.J., 2014. Architecture and composition of the Upper Burdigalian z-coral build-ups of southern Corsica (Mediterranean). Compt. Rendus Geosci. 346 (1–2), 45–51.
Gennari, R., Lozar, F., Turco, E., Dela Pierre, F., Lugli, S., Manzi, V., Natalicchio, M., Roveri, M., Schreiber, B.C., Taviani, M., 2018. Integrated stratigraphy and paleoceanographic evolution of the pre-evaporitic phase of the Messinian salinity crisis in the Eastern Mediterranean as recorded in the Tokhni section (Cyprus island). Newsl. Stratigr. 51 (1), 33–55.
Goldstein, S.J., Jacobsen, S.B., 1987. The Nd and Sr isotopic systematics of river-water dissolved material: Implications for the sources of Nd and Sr in seawater. Chem. Geol. Isot. Geosci. 66, 245–272.
Gueguen, E., Doglioni, C., Fernandez, M., 1998. On the post-25 Ma geodynamic evolution of the western Mediterranean. Tectonophysics 298, 259–269.
Halfar, J., Mutti, M., 2005. Global dominance of coralline red-algal facies: a response to Miocene oceanographic events. Geology 33 (6), 481–484.
Hallock, P., Schlager, W., 1986. Nutrient excess and the demise of coral reefs and carbonate platforms. Palaios 1 (4), 389–398.
Harzhauser, M., Kroh, A., Mandic, O., Piller, W.E., Göhlich, U., Reuter, M., Berning, B., 2007. Biogeographic responses to geodynamics: a key study all around the Oligo–Miocene Tethyan Seaway. Zool. Anzeiger-J. Comp. Zool. 246 (4), 241–256.
Henry, F., Jeandel, C., Dupre, B., Minster, J.F., 1994. Particulate and dissolved Nd in the western Mediterranean Sea: sources, fate and budget. Mar. Chem. 45 (4), 283–305.
Herbert, T.D., Lawrence, K.T., Tzanova, A., Peterson, L.C., Caballero-Gill, R., Kelly, C.S., 2016. Late Miocene global cooling and the rise of modern ecosystems. Nat. Geosci. 9 (11), 843–847.
Holbourn, A., Kuhnt, W., Simo, J.T., Li, Q., 2004. Middle Miocene isotope stratigraphy and paleoceanographic evolution of the northwest and southwest Australian margins (Wombat Plateau and Great Australian Bight). Palaeogeogr. Palaeoclimatol. Palaeoecol. 208 (1–2), 1–22.
Holbourn, A., Kuhnt, W., Schulz, M., Flores, J.A., Andersen, N., 2007. Orbitally-paced climate evolution during the middle Miocene "Monterey" carbon-isotope excursion. Earth Planet. Sci. Lett. 261 (3–4), 534–550.
Holbourn, A., Kuhnt, W., Clemens, S., Prell, W., Andersen, N., 2013. Middle to late Miocene stepwise climate cooling: Evidence from a high-resolution deep water isotope curve spanning 8 million years. Paleoceanography 28 (4), 688–699.
Holbourn, A.E., Kuhnt, W., Clemens, S.C., Kochhann, K.G., Jöhnck, J., Lübbers, J., Andersen, N., 2018. Late Miocene climate cooling and intensification of southeast Asian winter monsoon. Nat. Commun. 9 (1), 1–13.
Hüsing, S.K., Zachariasse, W.J., Van Hinsbergen, D.J., Krijgsman, W., Inceöz, M., Harzhauser, M., Mandic, O., Kroh, A., 2009. Oligocene–Miocene basin evolution in SE Anatolia, Turkey: constraints on the closure of the eastern Tethys gateway. Geol. Soc. Lond., Spec. Publ. 311 (1), 107–132.
Ingram, B.L., Sloan, D., 1992. Strontium isotopic composition of estuarine sediments as paleosalinity-paleoclimate indicator. Science 255, 68–72.
Jacobs, E., Weissert, H., Shields, G., Stille, P., 1996. The Monterey event in the Mediterranean: a record from shelf sediments of Malta. Paleoceanography 11 (6), 717–728.
James, N.P., 1997. The cool-water carbonate depositional realm. In: James, N.P., Clarke, J.A.D. (Eds.), Cool-water carbonates, SEPM Special Publication, vol. 56, pp. 1–20.
Janson, X., Eberli, G.P., Bonnaffe, F., Gaumet, F., De Casanove, V., 2007. Seismic expressions of a Miocene prograding carbonate margin, Mut Basin, Turkey. AAPG Bull. 91 (5), 685–713.
John, C.M., Mutti, M., Adatte, T., 2003. Mixed carbonate-siliciclastic record on the North African margin (Malta)—coupling of weathering processes and mid Miocene climate. Geol. Soc. Am. Bull. 115 (2), 217–229.
Karami, M.P., Meijer, P.T., Dijkstra, H.A., Wortel, M.J.R., 2009. An oceanic box model of the Miocene Mediterranean Sea with emphasis on the effects of closure of the eastern gateway. Paleoceanography 24 (4).
Kiessling, W., Flügel, E., Golonka, J., 1999. Paleoreef maps: evaluation of a comprehensive database on Phanerozoic reefs. AAPG Bull. 83 (10), 1552–1587.
Kocsis, L., Vennemann, T.W., Fontignie, D., Baumgartner, C., Montanari, A., Jelen, B., 2008. Oceanographic and climatic evolution of the Miocene Mediterranean deduced from Nd, Sr, C, and O isotope compositions of marine fossils and sediments. Paleoceanography 23 (4).
Kocsis, L., Vennemann, T.W., Hegner, E., Fontignie, D., Tütken, T., 2009. Constraints on Miocene oceanography and climate in the Western and Central Paratethys: O-, Sr-, and Nd-isotope compositions of marine fish and mammal remains. Palaeogeogr. Palaeoclimatol. Palaeoecol. 271 (1–2), 117–129.
Kouwenhoven, T.V., Van der Zwaan, G.J., 2006. A reconstruction of late Miocene Mediterranean circulation patterns using benthic foraminifera. Palaeogeogr. Palaeoclimatol. Palaeoecol. 238 (1–4), 373–385.
Lacan, F., Tachikawa, K., Jeandel, C., 2012. Neodymium isotopic composition of the oceans: A compilation of seawater data. Chem. Geol. 300, 177–184.
Lear, C.H., Rosenthal, Y., Coxall, H.K., Wilson, P.A., 2004. Late Eocene to early Miocene ice sheet dynamics and the global carbon cycle. Paleoceanography 19 (4).
Liebrand, D., Lourens, L.J., Hodell, D.A., Boer, B.D., Van de Wal, R.S.W., Pälike, H., 2011. Antarctic ice sheet and oceanographic response to eccentricity forcing during the early Miocene. Clim. Past 7 (3), 869–880.
Lustrino, M., Morra, V., Fedele, L., Franciosi, L., 2009. Beginning of the Apennine subduction system in central western Mediterranean: Constraints from Cenozoic "orogenic" magmatic activity of Sardinia, Italy. Tectonics 28 (5).
Mader, D., Montanari, A., Gattacceca, J., Koeberl, C., Handler, R., Coccioni, R., 2001. $^{40}Ar/^{39}Ar$ dating of a Langhian biotite–rich clay layer in the pelagic sequence of the Conero Riviera, Ancona, Italy. Earth Planet. Sci. Lett. 194, 111–126.
Manzi, V., Gennari, R., Hilgen, F., Krijgsman, W., Lugli, S., Roveri, M., Sierro, F.J., 2013. Age refinement of the Messinian salinity crisis onset in the Mediterranean. Terra Nova 25, 315–322.
Martín, J.M., Braga, J.C., Betzler, C., Brachert, T., 1996. Sedimentary model and high-frequency cyclicity in a Mediterranean, shallow-shelf, temperate-carbonate environment (uppermost Miocene, Agua Amarga Basin, Southern Spain). Sedimentology 43 (2), 263–277.
Martín, J.M., Braga, J.C., Aguirre, J., Puga-Bernabéu, Á., 2009. History and evolution of the North-Betic Strait (Prebetic Zone, Betic Cordillera): a narrow, early Tortonian, tidal-dominated, Atlantic–Mediterranean marine passage. Sediment. Geol. 216, 80–90.
Mateu-Vicens, G., Hallock, P., Brandano, M., 2008. A depositional model and paleoecological reconstruction of the lower Tortonian distally steepened ramp of Menorca (Balearic Islands, Spain). Palaios 23 (7), 465–481.
McArthur, J.M., Howarth, R.J., 2004. Strontium isotope stratigraphy. In: Gradstein, F., Ogg, J., Smith, A. (Eds.), A Geologic Time Scale. Cambridge University Press, Cambridge, pp. 96–105.
McArthur, J.M., Howarth, R.J., Bailey, T.R., 2001. Strontium isotope stratigraphy: LOWESS version 3—Best fit to the marine Sr-isotope curve for 0–509 Ma and accompanying look-up table for deriving numerical age. J. Geol. 109, 155–170.
McArthur, J.M., Howarth, R.J., Schields, G.A., 2012. Strontium isotope stratigraphy. In: Gradstein, F.M., et al. (Eds.), The Geologic Time Scale 2012. Elsevier, Amsterdam, pp. 207–232.
Meulenkamp, J.E., Sissingh, W., 2003. Tertiary palaeogeography and tectonostratigraphic evolution of the Northern and Southern Peri-Tethys platforms and the intermediate domains of the African–Eurasian convergent plate boundary zone. Palaeogeogr. Palaeoclimatol. Palaeoecol. 196 (1–2), 209–228.
Miller, K.G., Wright, J.D., Fairbanks, R.G., 1991. Unlocking the ice house: Oligocene-Miocene oxygen isotopes, eustasy, and margin erosion. J. Geophys. Res. 96, 6829–6848.
Montanari, A., Bice, D.M., Capo, R., Coccioni, R., Deino, A., DePaolo, D.J., Emmanuel, L., Monechi, S., Renard, M., Zevenboom, D., 1997a. Integrated stratigraphy of the Chattian to Mid-Burdigalian pelagic sequence of the Contessa Valley (Gubbio, Italy). In: Montanari, A., Odin, G.S., Coccioni, R. (Eds.), Miocene Stratigraphy: An Integrated Approach. Elsevier Science B.V, Amsterdam, Netherlands, pp. 249–277.
Montanari, A., Beaudoin, B., Chan, L.S., Coccioni, R., Deino, A., DePaolo, D.J., Emmanuel, L., Fornaciari, E., Kruge, M., Lundblad, S., Mozzato, C., Portier, E., Renard, M., Rio, D., Sandroni, P., Stankiewicz, A., 1997b. Integrated stratigraphy of the middle to upper Miocene pelagic sequence of Conero Riviera (Marche region, Italy). In: Montanari, A., Odin, G.S., Coccioni, R. (Eds.), Miocene Stratigraphy: An Integrated Approach. Elsevier Science B.V, Amsterdam, Netherlands, pp. 410–450.
Mutti, M., Bernoulli, D., 2003. Early marine lithification and hardground development on a Miocene ramp (Maiella, Italy): key surfaces to track changes in trophic resources in nontropical carbonate settings. J. Sediment. Res. 73 (2), 296–308.
Mutti, M., Hallock, P., 2003. Carbonate systems along nutrient and temperature gradients: some sedimentological and geochemical constraints. Int. J. Earth Sci. 92 (4), 465–475.
O'nions, R.K., Frank, M., Von Blanckenburg, F., Ling, H.F., 1998. Secular variation of Nd and Pb isotopes in ferromanganese crusts from the Atlantic, Indian and Pacific Oceans. Earth Planet. Sci. Lett. 155 (1), 15–28.
Pedley, M., 1996. Miocene reef facies of the Pelagian region (Central Mediterranean). In: Franseen, E.K., Esteban, M., Ward, W., Rouchy, J. (Eds.), Models for Carbonate Stratigraphy from Miocene Reef Complexes of Mediterranean Regions, vol. 5. SEPM Concepts in Sedimentology and Paleontology, Tulsa, pp. 247–260.
Pekar, S.F., DeConto, R.M., 2006. High-resolution ice-volume estimates for the early Miocene: Evidence for a dynamic ice sheet in Antarctica. Palaeogeogr. Palaeoclimatol. Palaeoecol. 231 (1–2), 101–109.
Perrin, C., Bosellini, F.R., 2013. The Late Miocene coldspot of z-coral diversity in the Mediterranean: patterns and causes. Comp. Rendus Palevol. 12 (5), 245–255.
Piepgras, D.J., Jacobsen, S.B., 1988. The isotopic composition of neodymium in the North Pacific. Geochim. Cosmochim. Acta 52 (6), 1373–1381.
Piepgras, D.J., Wasserburg, G.J., 1987. Rare earth element transport in the western North Atlantic inferred from Nd isotopic observations. Geochim. Cosmochim. Acta 51, 1257–1271.
Piepgras, D.J., Wasserburg, G.J., Dasch, E.J., 1979. The isotopic composition of Nd in different ocean masses. Earth Planet. Sci. Lett. 45 (2), 223–236.
Pomar, L., 1991. Reef geometries, erosion surfaces and high-frequency sea-level changes, upper Miocene Reef Complex, Mallorca, Spain. Sedimentology 38 (2), 243–269.
Pomar, L., 2001a. Types of carbonate platforms: a genetic approach. Basin Res. 13 (3), 313–334.
Pomar, L., 2001b. Ecological control of sedimentary accommodation: evolution from a carbonate ramp to rimmed shelf, Upper Miocene, Balearic Islands. Palaeogeogr. Palaeoclimatol. Palaeoecol. 175 (1–4), 249–272.

Pomar, L., Hallock, P., 2007. Changes in coral-reef structure through the Miocene in the Mediterranean province: adaptive versus environmental influence. Geology 35 (10), 899–902.
Pomar, L., Ward, W.C., Green, D.G., 1996. Upper Miocene reef complex of the Llucmajor area, Mallorca, Spain. In: Models for Carbonaie Stratigraphy from Miocene Reef Complexes of Mediterranean Regions, SEPM Concepts in Sedimentology and Paleontology, 5, pp. 191–225.
Pomar, L., Obrador, A., Westphal, H., 2002. Sub-wavebase cross-bedded grainstones on a distally steepened carbonate ramp, Upper Miocene, Menorca, Spain. Sedimentology 49 (1), 139–169.
Pomar, L., Brandano, M., Westphal, H., 2004. Environmental factors influencing skeletal grain sediment associations: a critical review of Miocene examples from the western Mediterranean. Sedimentology 51 (3), 627–651.
Pomar, L., Bassant, P., Brandano, M., Ruchonnet, C., Janson, X., 2012. Impact of carbonate producing biota on platform architecture: insights from Miocene examples of the Mediterranean region. Earth Sci. Rev. 113 (3–4), 186–211.
Pomar, L., Mateu-Vicens, G., Morsilli, M., Brandano, M., 2014. Carbonate ramp evolution during the late Oligocene (Chattian), Salento Peninsula, southern Italy. Palaeogeogr. Palaeoclimatol. Palaeoecol. 404, 109–132.
Pomar, L., Baceta, J.I., Hallock, P., Mateu-Vicens, G., Basso, D., 2017. Reef building and carbonate production modes in the west-central Tethys during the Cenozoic. Mar. Pet. Geol. 83, 261–304.
Popov, S.V., Rögl, F., Rozanov, A.Y., 2004. Lithological-paleogeographic maps of Paratethys. In: Popov, S.V., et al. (Eds.), Late Eocene to Pliocene, 250. Courier Forschungsinstitut Senckenberg, p. 46.
Rögl, F., 1999. Mediterranean and Paratethys: Facts and hypotheses of an Oligocene to Miocene paleogeography (short overview). Geol. Carpath. 50, 339–349.
Rohling, E.J., Marino, G., Grant, K.M., 2015. Mediterranean climate and oceanography, and the periodic development of anoxic events (sapropels). Earth Sci. Rev. 143, 62–97.
Ruchonnet, C., 2006. Climatic and oceanographic evolution of the Mediterranean basin during the late Serravallian/early Tortonian (middle/late Miocene): The record from the Ragusa Platform (SE Sicily, Italy). PhD Thesis. University of Geneva.
Ruchonnet, C., Kindler, P., 2010. Facies models and geometries of the Ragusa Platform (SE Sicily, Italy) near the Serravallian–Tortonian boundary. In: Carbonate Systems during the Oligocene-Miocene Climatic Transition, 42. IAS Spec. Publ, pp. 71–88.
Salocchi, A.C., Preto, N., Fontana, D., 2018. High-resolution chemostratigraphy of a Miocene wedge-top carbonate shelf (San Marino Fm., Northern Apennines, Italy): The major role of the Monterey global fertility event. Palaeogeogr. Palaeoclimatol. Palaeoecol. 505, 371–380.
Schildgen, T.F., Cosentino, D., Bookhagen, B., Niedermann, S., Yıldırım, C., Echtler, H., Wittmann, H., Strecker, M.R., 2012. Multi-phased uplift of the southern margin of the Central Anatolian plateau, Turkey: A record of tectonic and upper mantle processes. Earth Planet. Sci. Lett. 317, 85–95.
Schildgen, T.F., Cosentino, D., Frijia, G., Castorina, F., Dudas, F.Ö., Iadanza, A., Sampalmieri, G., Cipollari, P., Caruso, A., Bowring, S.A., Strecker, M.R., 2014. Sea level and climate forcing of the Sr isotope composition of late Miocene Mediterranean marine basins. Geochem. Geophys. Geosyst. 15, 2964–2983.
Schlager, W., 2005. Carbonate sedimentology and sequence stratigraphy. Concepts in Sedimentology and Paleontology, SEPM 8, 200 pp.
Simon, D., Palcu, D., Meijer, P., Krijgsman, W., 2019. The sensitivity of middle Miocene paleoenvironments to changing marine gateways in Central Europe. Geology 47 (1), 35–38.
Spivack, A.J., Wasserburg, G.J., 1988. Neodymium isotopic composition of the Mediterranean outflow and the eastern North Atlantic. Geochim. Cosmochim. Acta 52, 2767–2773.
Super, J.R., Thomas, E., Pagani, M., Huber, M., O'Brien, C., Hull, P.M., 2018. North Atlantic temperature and pCO_2 coupling in the early-middle Miocene. Geology 46 (6), 519–522.
Super, J.R., Thomas, E., Pagani, M., Huber, M., O'Brien, C.L., Hull, P.M., 2020. Miocene evolution of North Atlantic Sea surface temperature. Paleoceanogr. Paleoclimatol. 35 (5), e2019PA003748.
Tachikawa, K., Roy-Barman, M., Michard, A., Thouron, D., Yeghicheyan, D., Jeandel, C., 2004. Neodymium isotopes in the Mediterranean Sea: Comparison between seawater and sediment signals. Geochim. Cosmochim. Acta 68 (14), 3095–3106.
Tomassetti, L., Brandano, M., 2013. Sea level changes recorded in mixed siliciclastic–carbonate shallow-water deposits: The Cala di Labra Formation (Burdigalian, Corsica). Sediment. Geol. 294, 58–67.
Tomassetti, L., Bosellini, F.R., Brandano, M., 2013. Growth and demise of a Burdigalian coral bioconstruction on a granite rocky substrate (Bonifacio Basin, southeastern Corsica). Facies 59 (4), 703–716.
Tzanova, A., Herbert, T.D., Peterson, L., 2015. Cooling Mediterranean Sea surface temperatures during the Late Miocene provide a climate context for evolutionary transitions in Africa and Eurasia. Earth Planet. Sci. Lett. 419, 71–80.
Vescogni, A., Bosellini, F.R., Cipriani, A., Gürler, G., Ilgar, A., Paganelli, E., 2014. The Dağpazarı carbonate platform (Mut Basin, Southern Turkey): Facies and environmental reconstruction of a coral reef system during the Middle Miocene Climatic Optimum. Palaeogeogr. Palaeoclimatol. Palaeoecol. 410, 213–232.
Vincent, E., Berger, W.H., 1985. Carbon dioxide and polar cooling in the Miocene: the Monterey hypothesis. In: The Carbon Cycle and Atmospheric CO_2: Natural Variations Archean to Present, 32, pp. 455–468.
Westerhold, T., Bickert, T., Röhl, U., 2005. Middle to late Miocene oxygen isotope stratigraphy of ODP site 1085 (SE Atlantic): new constrains on Miocene climate variability and sea-level fluctuations. Palaeogeogr. Palaeoclimatol. Palaeoecol. 217 (3–4), 205–222.
Wilson, M.E.J., Vecsei, A., 2005. The apparent paradox of abundant foramol facies in low latitudes: their environmental significance and effect on platform development. Earth Sci. Rev. 69 (1–2), 133–168.
Woodruff, F., Savin, S., 1991. Mid-Miocene isotope stratigraphy in the deep sea: high-resolution correlations, paleoclimatic cycles, and sediment preservation. Paleoceanography 6, 755–806.
Wu, J., Pahnke, K., Böning, P., Wu, L., Michard, A., de Lange, G.J., 2019. Divergent Mediterranean seawater circulation during Holocene sapropel formation–Reconstructed using Nd isotopes in fish debris and foraminifera. Earth Planet. Sci. Lett. 511, 141–153.
You, Y., Huber, M., Müller, R.D., Poulsen, C.J., Ribbe, J., 2009. Simulation of the middle Miocene climate optimum. Geophys. Res. Lett. 36 (4).
Zachos, J., Pagani, M., Sloan, L., Thomas, E., Billups, K., 2001. Trends, rhythms, and aberrations in global climate 65 Ma to present. Science 292, 686–693.
Zachos, J.C., Dickens, G.R., Zeebe, R.E., 2008. An early Cenozoic perspective on greenhouse warming and carbon-cycle dynamics. Nature 451, 279–283.